

Large Eddy Simulation (LES) Applied to Advanced Engine Combustion Research

Joseph C. Oefelein and Guilhem Lacaze

**Combustion Research Facility
Sandia National Laboratories, Livermore, CA 94551**

**Support Provided by the DOE
Office of Energy Efficiency and Renewable Energy
Vehicle Technologies Office
is Gratefully Acknowledged**



Overview

Timeline

- Project provides fundamental research that supports advanced engine development
- Focused on next generation simulations, models, and workflow for model validation using Large Eddy Simulation
- Project scope, direction, and continuation evaluated annually

Budget

- Total Project Funding
 - FY15 – \$390K
 - FY16 – \$260K

Barriers

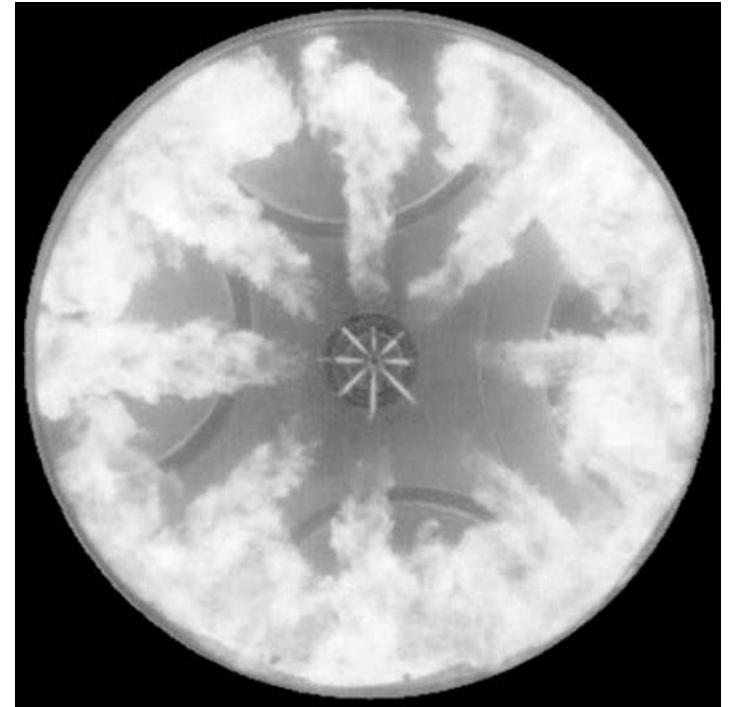
- Two sets of barriers addressed
 - 1 – Lack of fundamental knowledge of Diesel and GDI combustion regimes
 - Understanding coupled effects of fuel-injection, turbulent-mixing, heat-transfer, chemical-kinetics, and geometry on combustion and emissions over broad operating ranges
 - 2 – Lack of predictive models for engine combustion design and control
 - Efficient and routine use of advanced High-Performance-Computing (HPC) codes and computer architectures

Partners

- CRF Engine and UQ Groups
- Penn State, Stanford, Michigan CERFACS (e.g., DOE/NSF/FOA)
- DOE Office of Science
- Project Lead: Joe Oefelein

Relevance ... need for advanced model development is well recognized

- Combustion involves strongly coupled, multiscale/multiphysics phenomena
 - High-Reynolds-number turbulence and scalar-mixing processes ($Re \geq 100,000$)
 - High-pressure mixed-mode combustion
 - Compressible, acoustically active flow
 - Complex fuels, multiphase flow
 - Complex geometries
- Current models not predictive, no one research approach gives all of the data required for validation
 - Simulations only treat limited ranges of scales
 - Experiments provide limited information
 - Many sources of uncertainty
 - Costs can be prohibitive
- Consequence ... inconsistencies in model development demonstrated for years



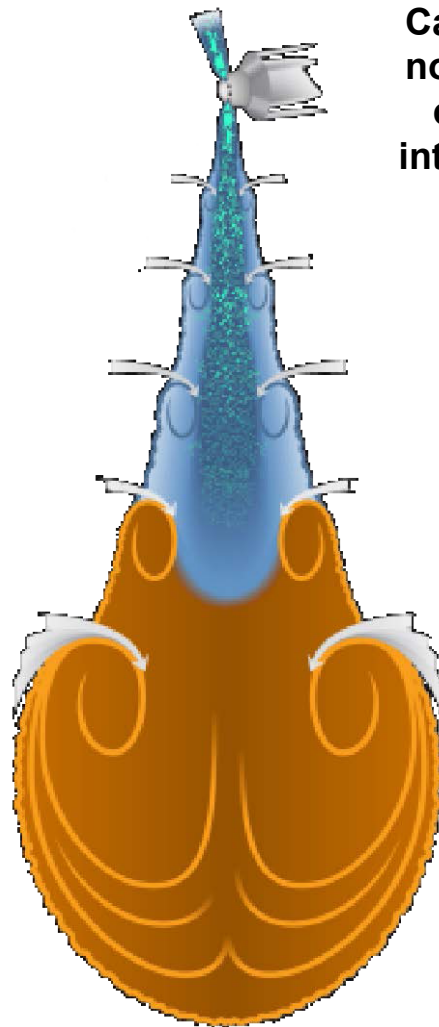
Diesel spray combustion imaging through transparent piston
(Mark Musculus, Sandia)

High-resolution LES combined with first principles models and UQ can provide next level of precision and data that complements experiments

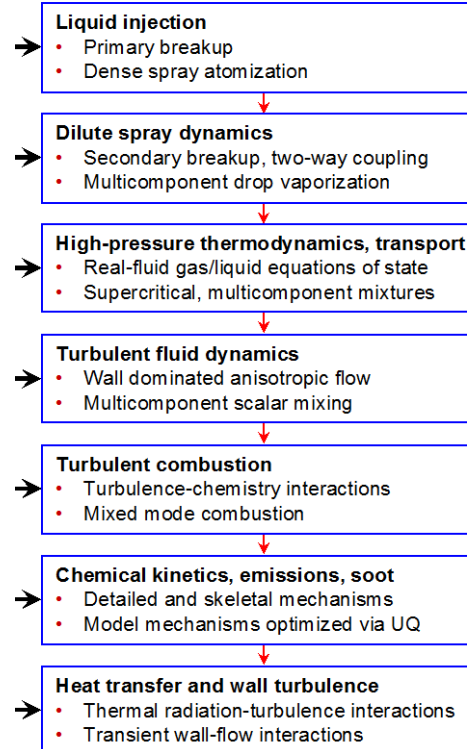
Challenges

- **Available data does not provide all the information required to draw distinguishing conclusions due to harsh environments**
 - Penetration, flame lift-off measurements necessary but not sufficient, instantaneous imaging is qualitative
 - Sub-model accuracy is difficult to assess due to coupling between models (e.g., injection → mixing → combustion → emissions)
- **Many uncertainties exist in addition to model accuracy**
 - Poor grid quality and/or lack of appropriate spatial or temporal resolution
 - Incorrect and/or ill-posed boundary conditions
 - Error-prone (dissipative) numerical methods
- **Net accuracy of simulations is complicated by**
 - Nonlinear interdependence between sub-models
 - Model variability and numerical implementation
 - Competition between model and numerical error
- **Combined uncertainties make it difficult to draw conclusions regarding both model performance and implementation requirements**

Approach ... address challenges using specialized LES solver with HPC

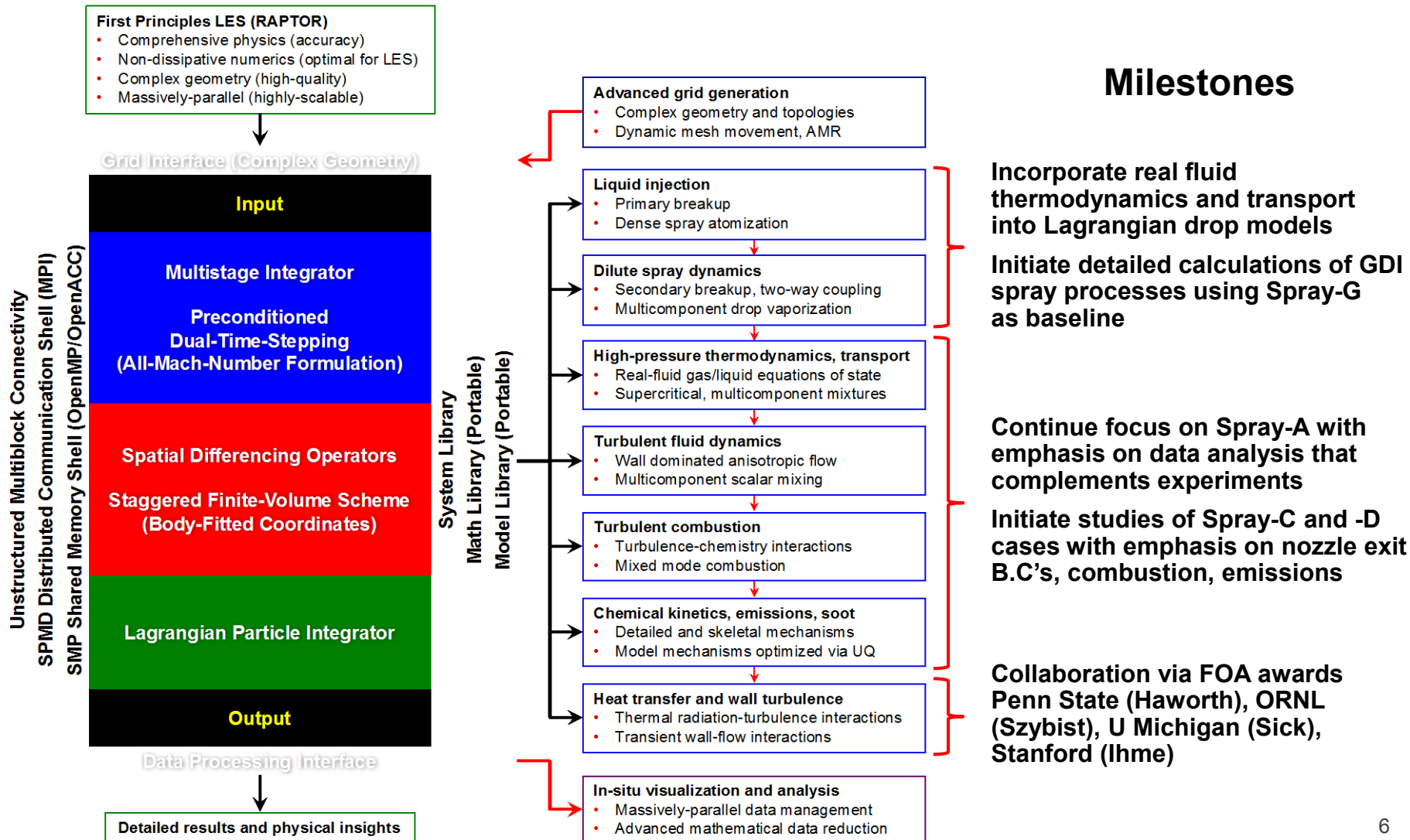


Cascade of nonlinearly coupled interactions

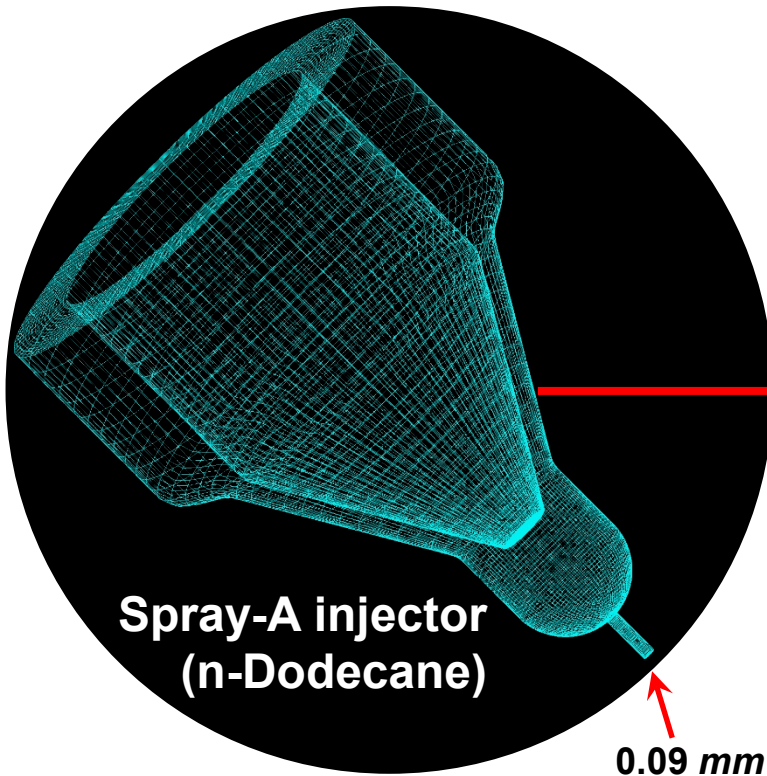


- **Focus on Diesel and GDI injection and combustion**
- **Perform progressive analysis of the coupled system of sub-models**
- **Complement advanced experiments with detailed LES**
- **Provide data and insights not available from experiments alone**

Approach ... address challenges using specialized LES solver with HPC



Established benchmark simulations for both Diesel and GDI cases; e.g.,



Injection Conditions

Temperature:	363 K
Density:	650 kg/m ³
Peak Velocity:	600 m/s
Peak Re _d :	120,000

Sandia High-Pressure Combustion Vessel

Initial Conditions

Pressure: 60 bar

Temperature: 900K

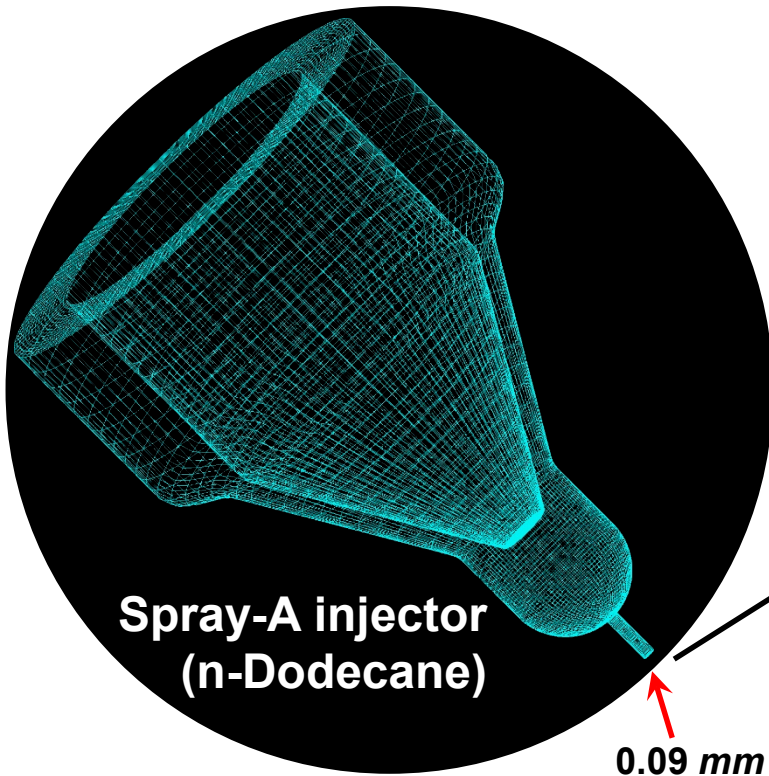
Composition: 15% O₂

1050 d

1080 d

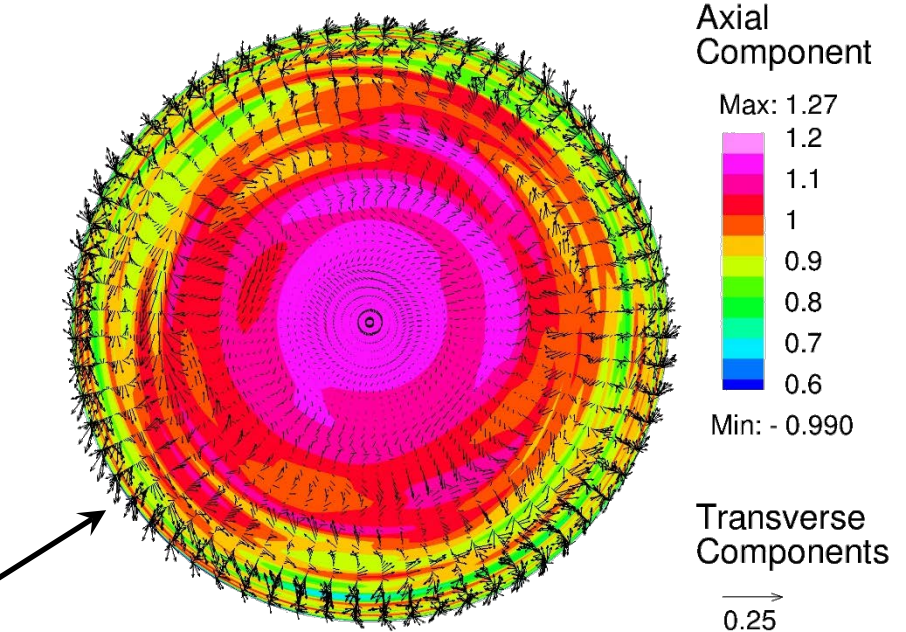
Detailed treatment of geometry and boundary conditions, 2μm grid spacing

Methodology to approximate complex boundary layer dynamics validated



Injection Conditions

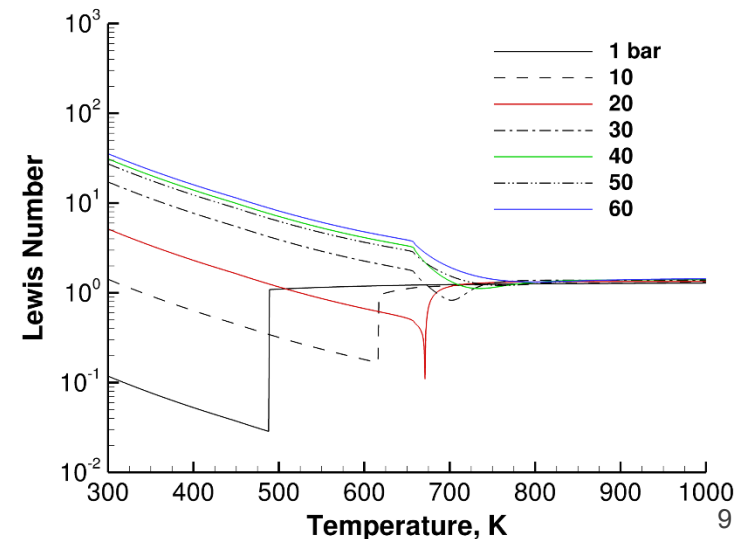
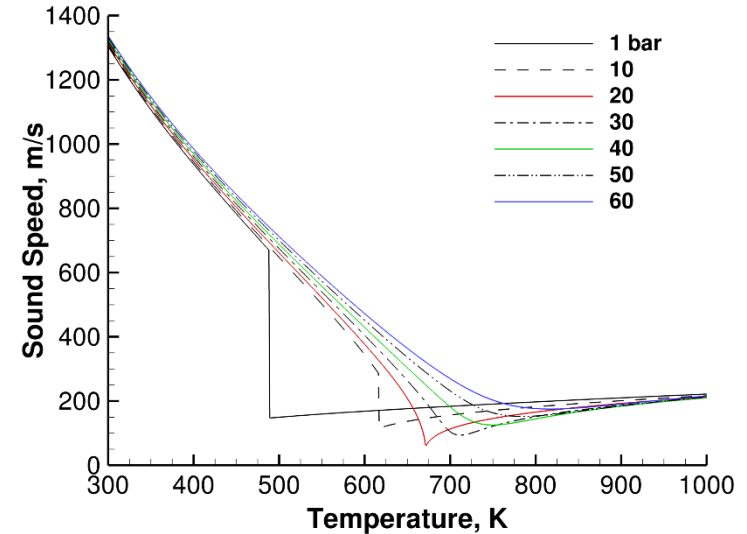
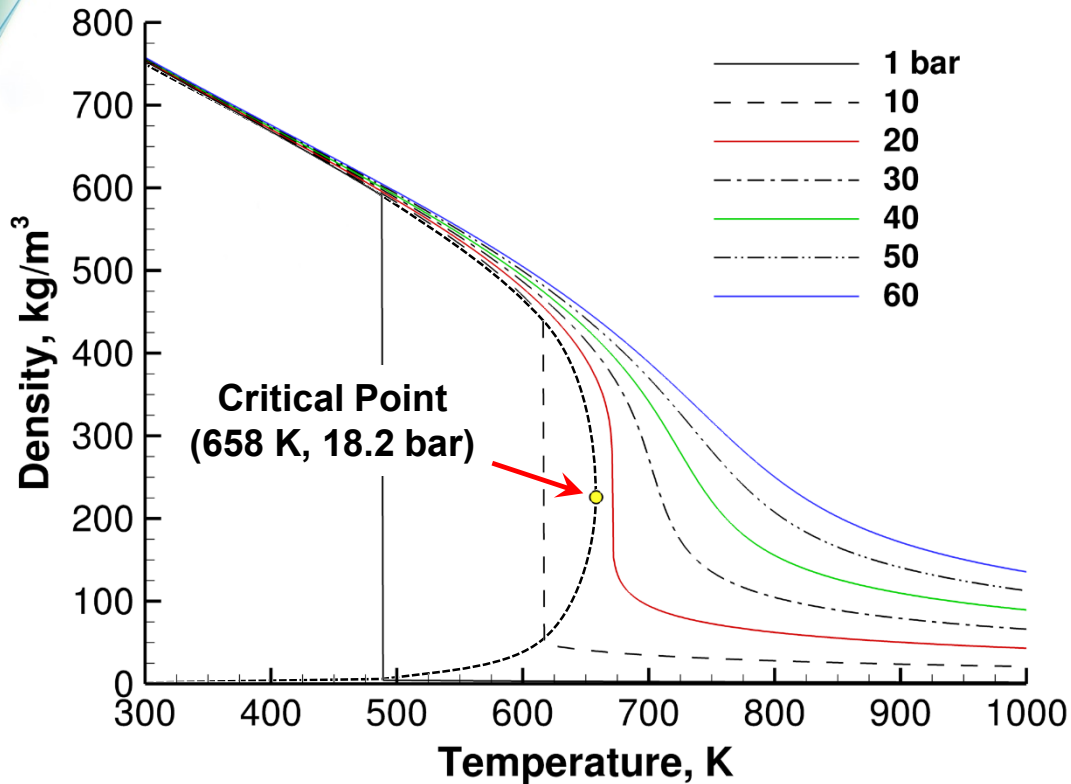
Peak Velocity: 600 m/s
 Peak Re_d : 117,000
 Density: 650 kg/m³
 Temperature: 363 K



Time-evolving turbulent boundary layer dynamics reconstructed using Synthetic Eddy Method (Jarrin et al., 2008)

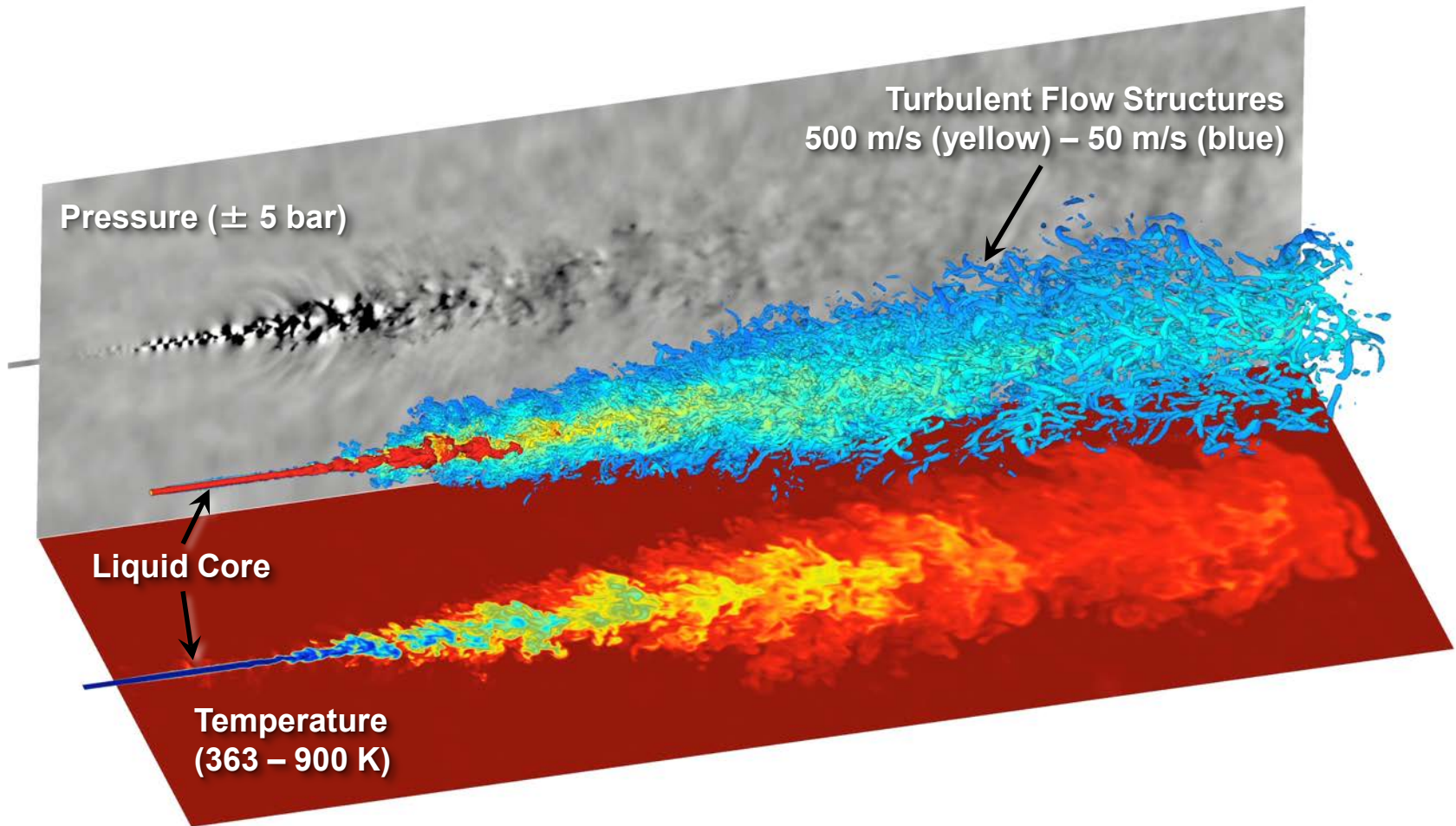
- Uses assumed, measured, or calculated turbulence properties as input (integral scale distribution, Reynolds stress tensor, and mean velocity profile)
- Facilitates quantified control of inflow boundary conditions for anisotropic, nonequilibrium, rough wall conditions, etc.

Detailed treatment of properties for hydrocarbon fuels demonstrated



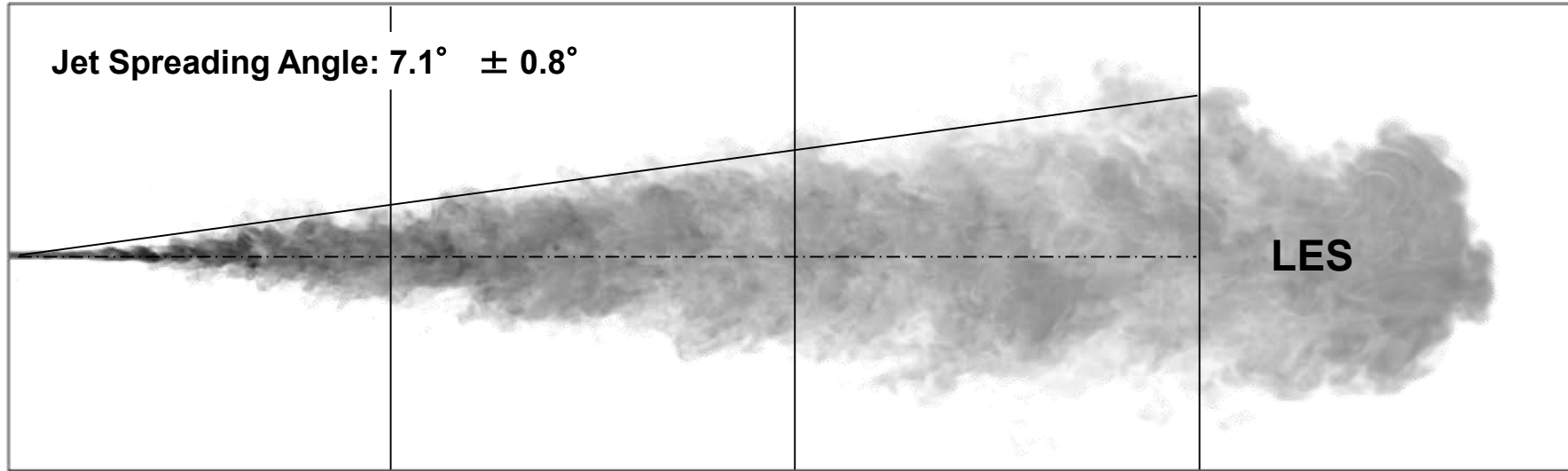
- Real-fluid mixture properties obtained using Extended Corresponding States model
- Multicomponent formulation using cubic (PR/SRK) or BWR equations of state
- Generalized to treat wide range of hydrocarbon mixtures (Fuel/Oxidizer/Products)

Fully-coupled implementation of sub-models quantifies details of mixing



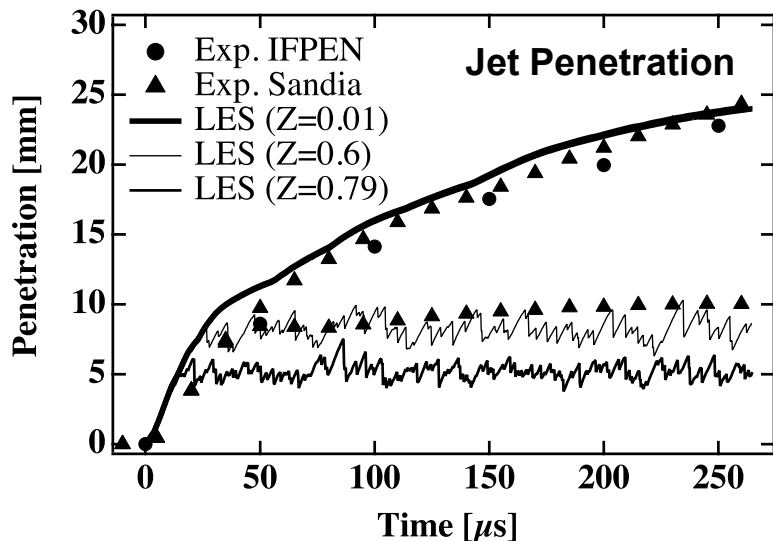
Demonstrated good agreement with available data with no tuned constants

3



-3

0

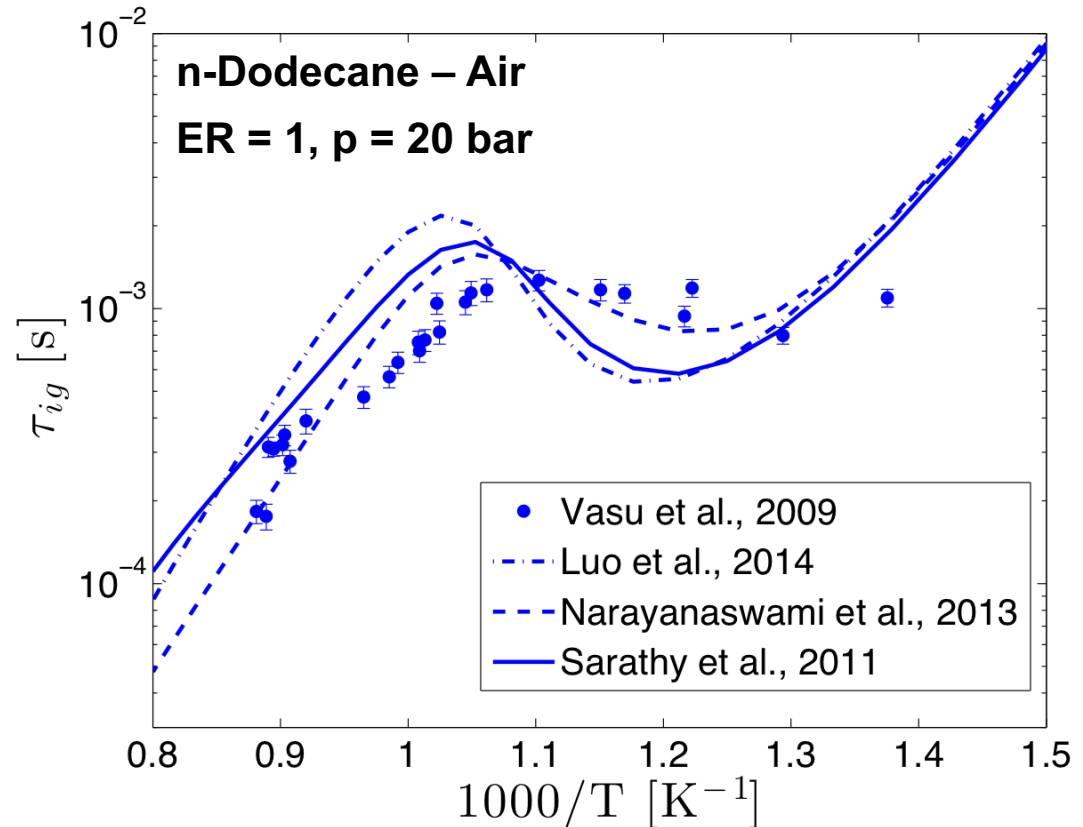


- Analysis of data not available from experiment provides additional insights:
 - e.g., Transient mixture state over range of times just prior to autoignition
- Identification of flammable regions quantifies conditions where the chemical model must perform accurately
 - Temperature, K ($700 < T < 900$)
 - Equivalence Ratio ($0.5 < \Phi < 4$)
 - Pressure: 60 ± 5 bar

18

Highlighted the inherent variability in chemical mechanisms

- Sarathy et al., 2011
 - 2-methyl-alkanes and n-alkanes up to C12
 - 2755 species
 - 11173 reactions
- Narayanaswami et al., 2013
 - Skeletal mechanism
 - 255 species
 - 2289 reactions
- Luo et al., 2014
 - Skeletal mechanism
 - 105 species
 - 420 reactions
- All designed for up to 20 bar, 600 – 1500 K



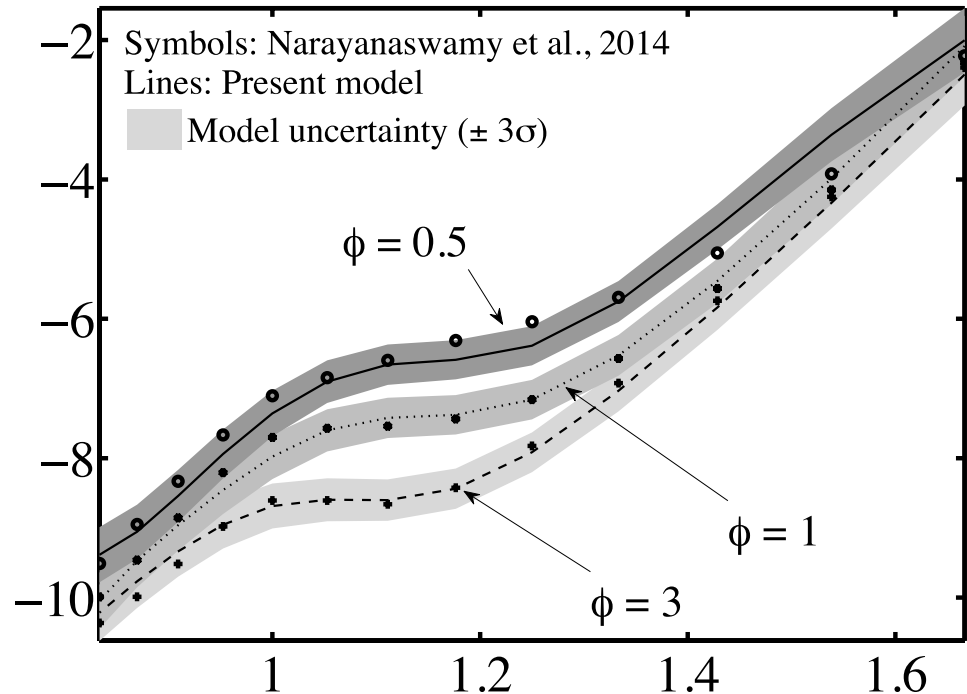
Used UQ to derive optimized chemical models that balance variability vs. cost

- **Objective:**

- Design for specified range of operating conditions (p, T, ϕ) using selected reference mechanism
- Optimize to capture specific chemical characteristics (e.g., ignition delay, flame propagation, selected emissions)
- Determine least expensive model that provides selected characteristics with error bars on prediction

- **Approach:**

- Start with simplest model form; e.g., Arrhenius based equations (Westbrook et al. 1981, Misdariis et al. 2014)
- Functionalize pre-exponential factors and activation energies w.r.t. p, T, ϕ
- Use Bayesian inference to fit most probable surfaces over specified ranges



L. Hakim, G. Lacaze, M. Khalil, H. N. Najm, and J. C. Oefelein. Modeling auto-ignition transients in reacting diesel jets. *Journal of Engineering for Gas Turbines and Power*, **138**:112806, 2016.

L. Hakim, G. Lacaze, M. Khalil, K. Sargsyan, H. N. Najm, and J. C. Oefelein. Probabilistic parameter estimation of a 2-step chemical kinetics model for n-dodecane jet autoignition. *Combustion Theory and Modelling*, Submitted.



Demonstrated merits of combustion closure via stochastic reconstruction

- Filtered chemical source terms evaluated using space-time filtering with modeled instantaneous scalar field, $\phi_i(\mathbf{x}, t)$; i.e.,

$$\bar{\dot{\omega}}_i(\mathbf{x}, t) = \int_t^{t+\Delta t} \left\{ \iiint_{V(\tau)} \mathcal{G}(\mathbf{y} - \mathbf{x}, \tau - t; \delta \mathbf{y}, \delta \tau) \dot{\omega}_i(\phi_1, \phi_2, \dots; \mathbf{y}, \tau) dV \right\} d\tau$$

where

$$\phi_i(\mathbf{x}, t) = \tilde{\phi}_i(\mathbf{x}, t) + \phi_i''(\mathbf{x}, t)$$

- Correlated scalar fluctuations generated stochastically using Cholesky decomposition
 1. Requires subfilter variance/covariance matrix as input
 2. Obtained using approximate deconvolution model with assumed scalar spectrum
- Modeled instantaneous signal used to evaluate filtered chemical source terms directly
 1. Fluctuations generated asynchronously on subfilter-scale in time at frequencies consistent with local eddy lifetimes and transit times
 2. Taylor's hypothesis coupled with local convective CFL number provides relation between spatial and temporal filtering

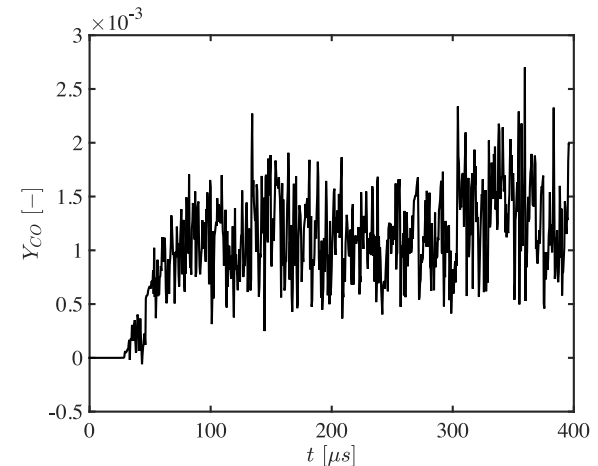
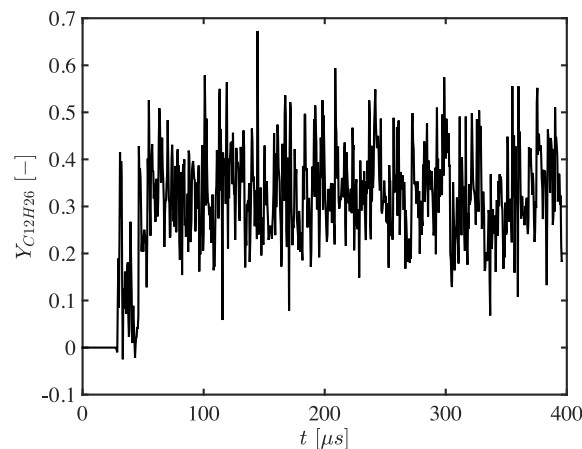
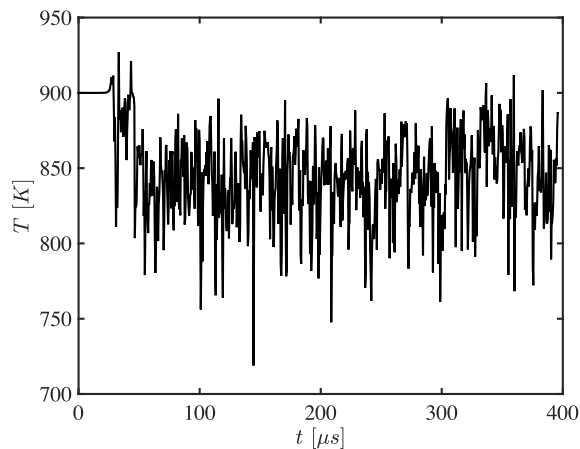
Demonstrated merits of combustion closure via stochastic reconstruction

- Filtered chemical source terms evaluated using space-time filtering with modeled instantaneous scalar field, $\phi_i(\mathbf{x}, t)$; i.e.,

$$\bar{\dot{\omega}}_i(\mathbf{x}, t) = \int_t^{t+\Delta t} \left\{ \iiint_{V(\tau)} \mathcal{G}(\mathbf{y}-\mathbf{x}, \tau-t; \delta\mathbf{y}, \delta\tau) \dot{\omega}_i(\phi_1, \phi_2, \dots; \mathbf{y}, \tau) dV \right\} d\tau$$

where

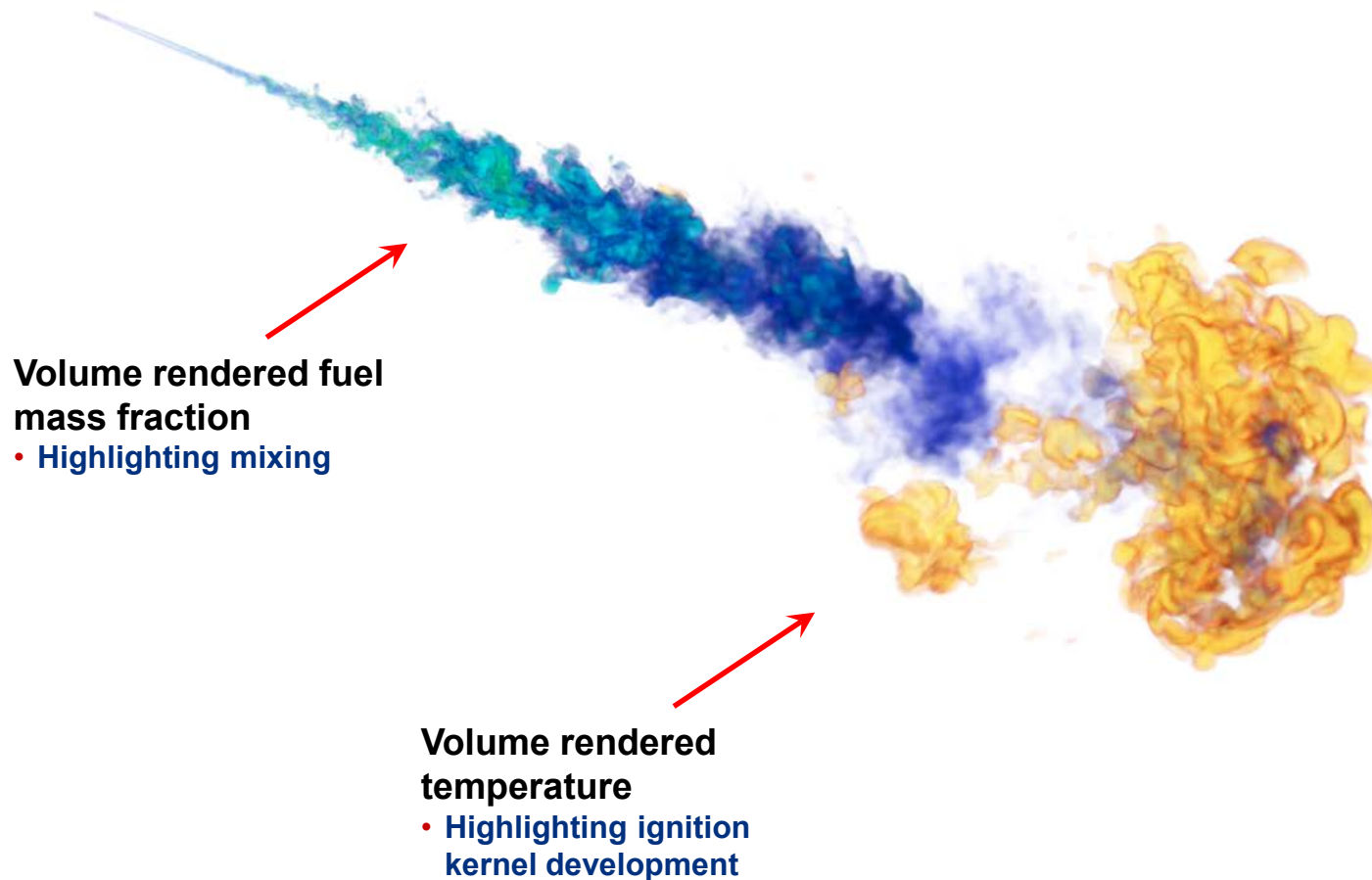
$$\phi_i(\mathbf{x}, t) = \tilde{\phi}_i(\mathbf{x}, t) + \phi_i''(\mathbf{x}, t)$$



e.g., Modeled instantaneous scalars on center line at 100 diameters (Spray A)

Combination of models provides details that complement experiments

L. Hakim, G. Lacaze, and J. C. Oefelein. Large eddy simulation of autoignition transients in a model Diesel injector configuration. *SAE World Congress*, Paper 2016-01-0872, April 12-14, 2016.



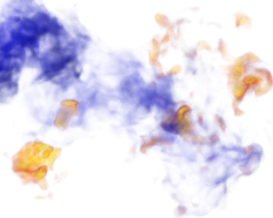
Ignition sequence

$t=220 \mu\text{s}$



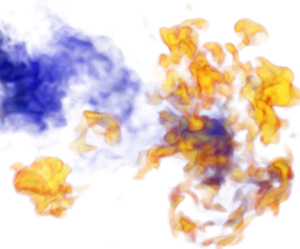
First kernel, diameter $\approx 500 \mu\text{m}$ (too small to be optically detected in experiment)
Location: tip of the jet, off-axis

$t=250 \mu\text{s}$

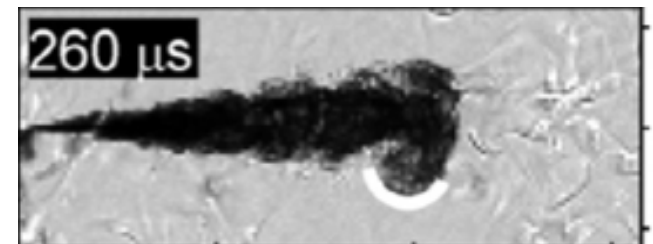


Independent kernels appear, diameter $\approx 500 \mu\text{m}$ to 2mm (still very small for optical detection)
Location: tip of the jet, off-axis

$t=270 \mu\text{s}$



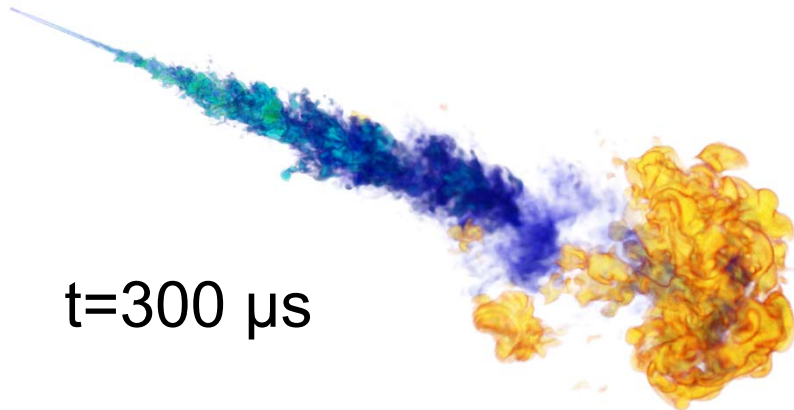
Many small kernels present in the “jet tip” region ... impact on Schlieren?



Schlieren images by Skeen *et al.*, PCI, 2015

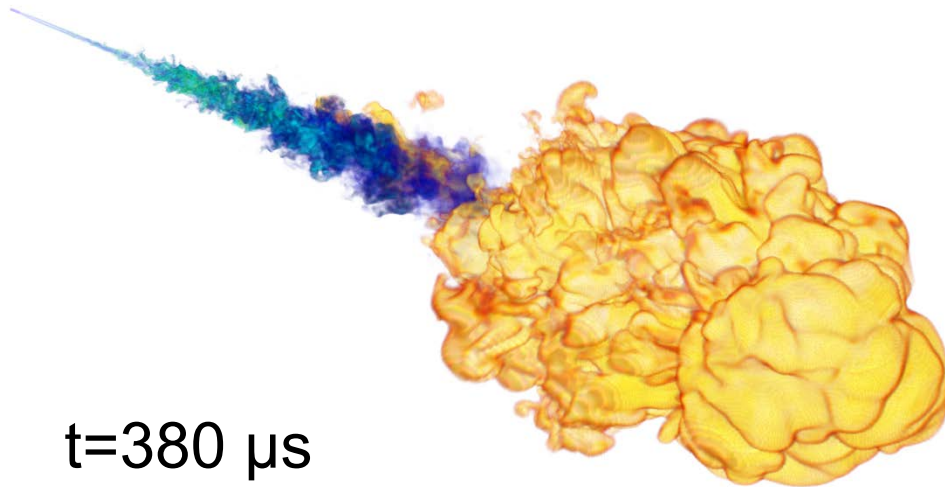
Ignition sequence

$t=300 \mu\text{s}$

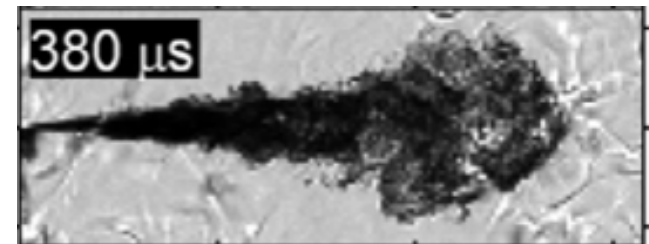


Single flame structure with upstream independent kernels, flame expands through dilatation and autoignition

$t=380 \mu\text{s}$



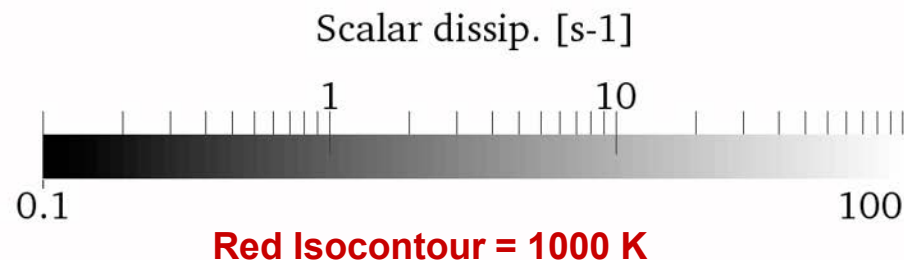
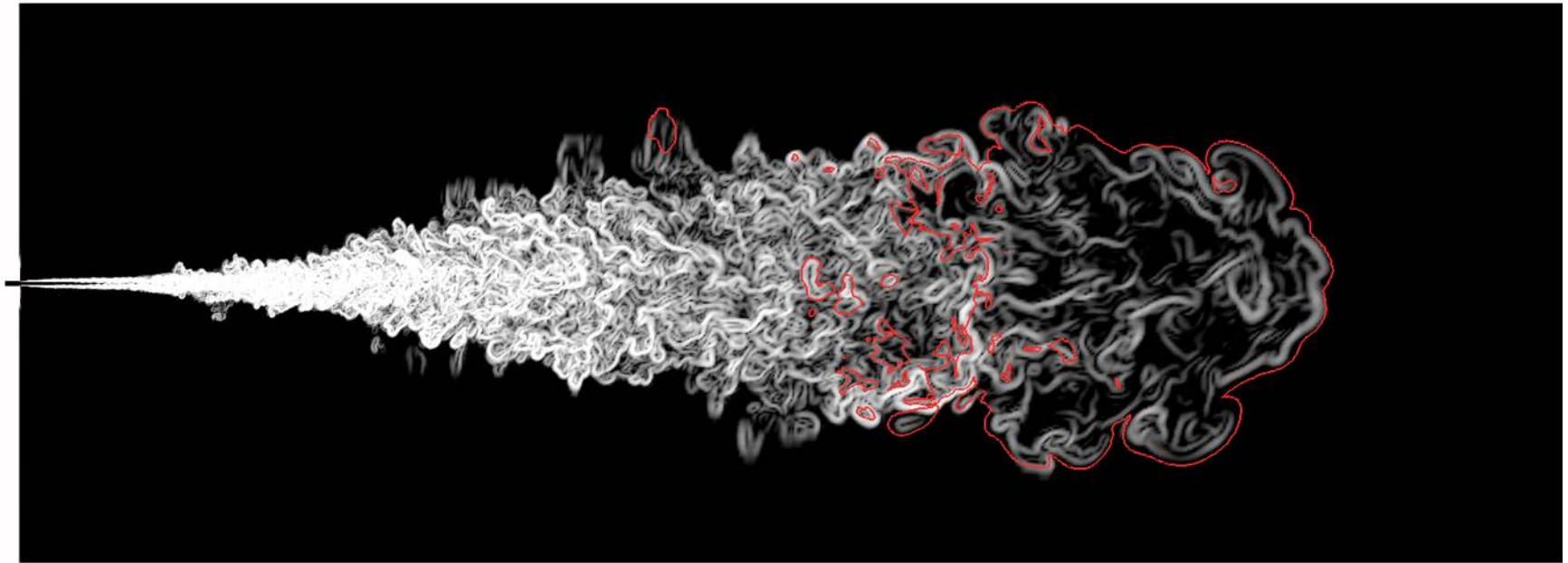
Main flame region at the jet extremity, autoignition locations observed ahead of main front



Schlieren images by Skeen *et al.*, PCI, 2015

Currently using the Spray-A benchmark to extract data that can't be measured

e.g., 3D high-repetition flow-flame interactions, dynamics of scalar dissipation, etc.



Same approach now being applied for GDI sprays (Lagrangian-Eulerian)



Photo courtesy C. F. Edwards, Stanford University

1. Primary atomization (sheet, filament and lattice formation)

2. Secondary breakup (including particle deformation, coalescence)

3. Dilute spray dynamics

- a. Drop dispersion
- b. Multicomponent drop vaporization
- c. Two-way coupling between gas and dispersed liquid phase
 - Turbulence modulation (damping of turbulence due to particle drag effects)
 - Turbulence generation (production of turbulence due to particle wakes)

A new dense spray formulation based on space-time filtering has been implemented

Current focus is on advanced treatment of secondary breakup and dilute spray dynamics

4. Turbulent mixed-mode combustion

- a. Complex high-pressure hydrocarbon chemistry
- b. Emissions and soot

Formulation includes detailed modeling of filtered void fraction, source terms

- Mass:

$$\frac{\partial}{\partial t}(\theta \bar{\rho}) + \nabla \cdot (\theta \bar{\rho} \tilde{\mathbf{u}}) = \bar{\dot{\rho}}_s$$

- Momentum:

$$\frac{\partial}{\partial t}(\theta \bar{\rho} \tilde{\mathbf{u}}) + \nabla \cdot \left[\theta \left(\bar{\rho} \tilde{\mathbf{u}} \otimes \tilde{\mathbf{u}} + \frac{\mathcal{P}}{M^2} \mathbf{I} \right) \right] = \nabla \cdot (\theta \vec{\mathcal{T}}) + \bar{\mathbf{F}}_s$$

- Total Energy:

$$\frac{\partial}{\partial t}(\theta \bar{\rho} \tilde{e}_t) + \nabla \cdot [\theta (\bar{\rho} \tilde{e}_t + \mathcal{P}) \tilde{\mathbf{u}}] = \nabla \cdot \left[\theta \left(\vec{\mathcal{Q}}_e + M^2 (\vec{\mathcal{T}} \cdot \tilde{\mathbf{u}}) \right) \right] + \theta \bar{\mathcal{Q}}_e + \bar{\mathcal{Q}}_s$$

- Species:

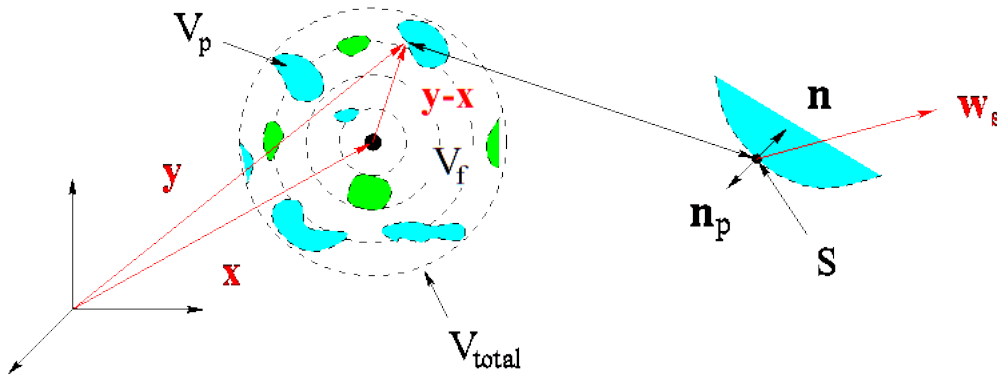
$$\frac{\partial}{\partial t}(\theta \bar{\rho} \tilde{Y}_i) + \nabla \cdot (\theta \bar{\rho} \tilde{Y}_i \tilde{\mathbf{u}}) = \nabla \cdot (\theta \vec{\mathcal{S}}_i) + \theta \bar{\dot{\omega}}_i + \bar{\dot{\omega}}_{s_i}$$

- Spray Source Terms
- Composite Stresses/Fluxes
- Chemical Source Terms

Formulation includes detailed modeling of filtered void fraction, source terms

$$\overline{\mathcal{H}}_s(\mathbf{x}, t) = \underbrace{\int_t^{t+\Delta t} \sum_p \mathcal{G}(\mathbf{y}_p - \mathbf{x}, \tau - t)}_{(iii)} \underbrace{\left\{ \underbrace{\oint \oint_{S(\mathbf{y}_p, \tau)} \vec{\psi}(\mathbf{y}_p, \tau) \cdot \mathbf{n}_p dS}_{(i)} \right\}}_{(ii)} d\tau$$

- (i) Instantaneous rate of exchange across drop interfaces at remote points \mathbf{y}_p and times τ
(ii) Spatially filtered effect of remote exchange processes on discrete points \mathbf{x} at times τ
(iii) Filtered effect of temporal disturbances that occur over the interval $t \leq \tau \leq t + \Delta t$

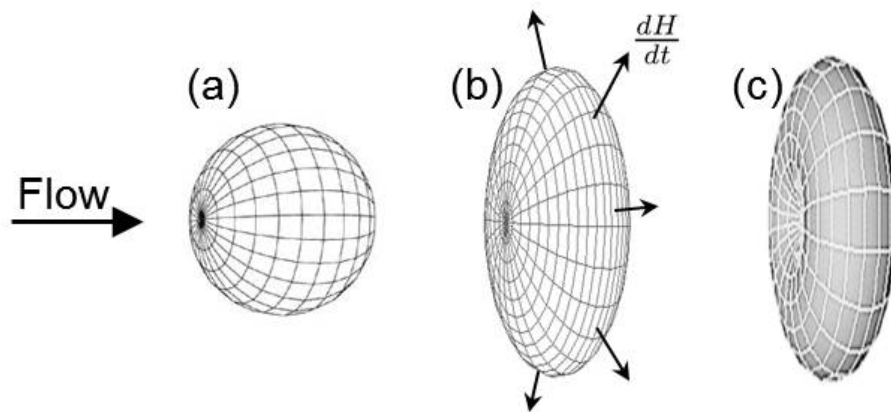
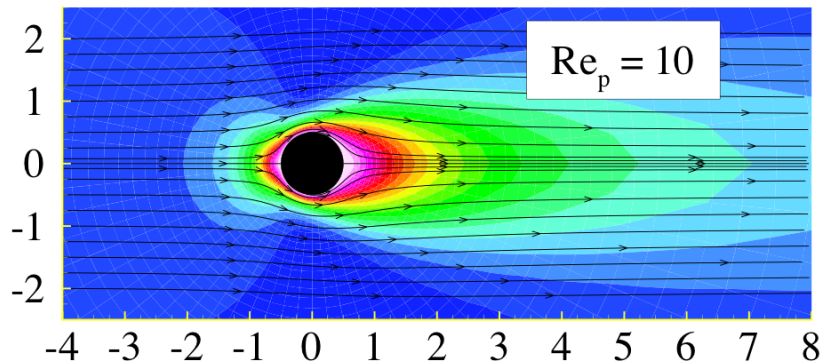


$\overline{\mathcal{H}}_s(\mathbf{x}, t)$	$\oint \oint_{S(\mathbf{y}_p, \tau)} \vec{\psi}(\mathbf{y}_p, \tau) \cdot \mathbf{n}_p dS$
$\overline{\rho}_s(\mathbf{x}, t)$	$-\left\{ \frac{dm_p}{d\tau} \right\}$
$\overline{\mathbf{F}}_s(\mathbf{x}, t)$	$-\left\{ \frac{dm_p}{d\tau} \mathbf{u}_p + m_p \frac{d\mathbf{u}_p}{d\tau} \right\}$
$\overline{Q}_s(\mathbf{x}, t)$	$-\left\{ \frac{dm_p}{d\tau} e_{tp} + m_p \frac{de_{tp}}{d\tau} \right\}$
$\overline{\dot{\omega}}_{s_i}(\mathbf{x}, t)$	$-\left\{ \frac{dm_p}{d\tau} Y_{ip} + m_p \frac{dY_{ip}}{d\tau} \right\}$

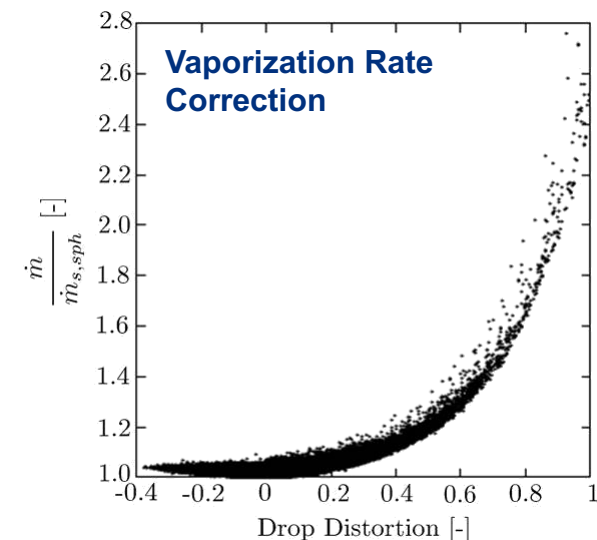
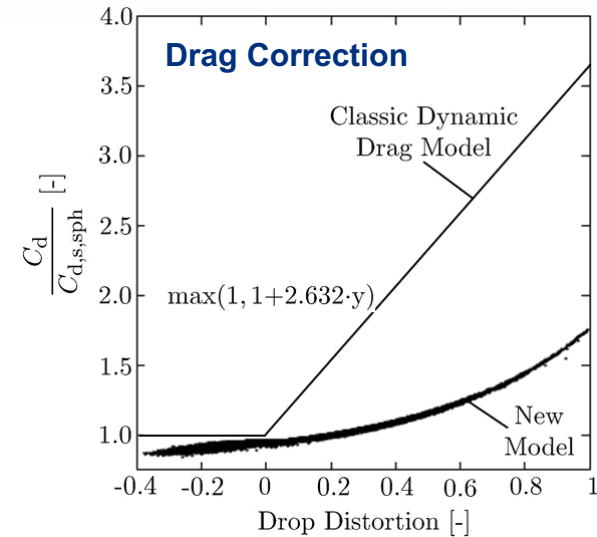
- Form of source terms derived through mathematical formalism of LES using time-dependent filter kernel
- Drop mass, volume, and (assumed) topology are accounted for (e.g., no need to assume “point particle limit”)
- Lagrangian ODE’s (drop dynamics) integrated on subfilter time scales using modeled instantaneous scalar field (consistent with stochastic reconstruction model used in combustion closure) ... no adjustable constants

Sensitizing drops to subfilter time scales facilitates model improvements

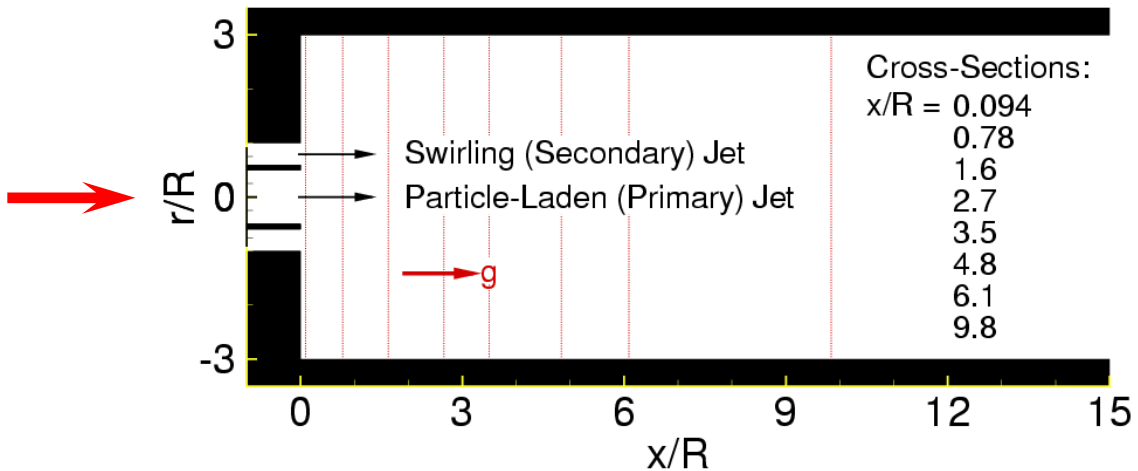
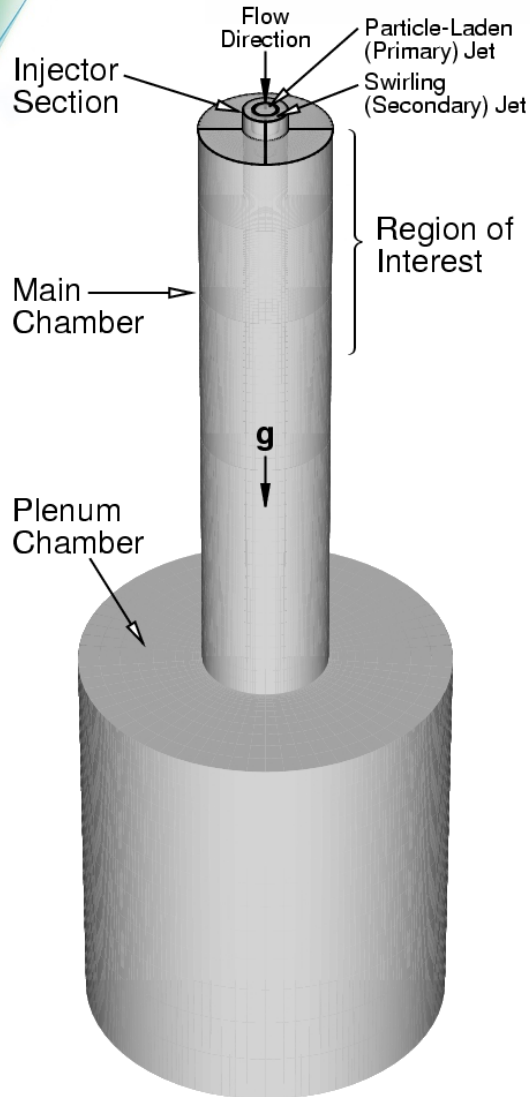
- Physical drops (not parcels) are tracked
- System of drop models (e.g., drag, vaporization) now modified to include drop non-sphericity



R. N. Dahms and J. C. Oefelein. The significance of drop non-sphericity in sprays. *International Journal of Multiphase Flow*, **86**:67–85, 2016.

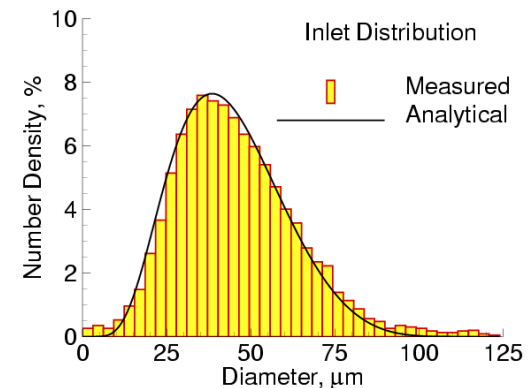


Baseline closure has been systematically validated

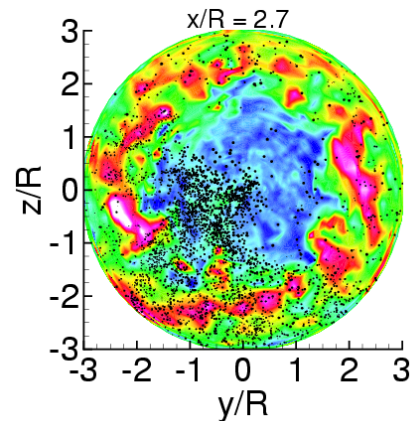
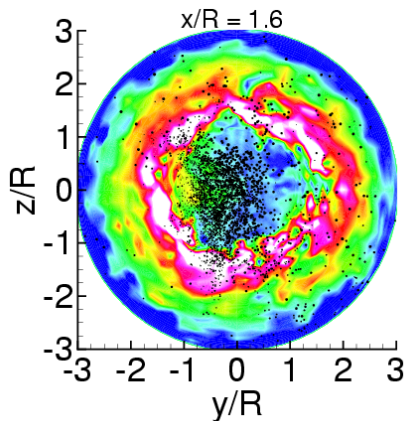
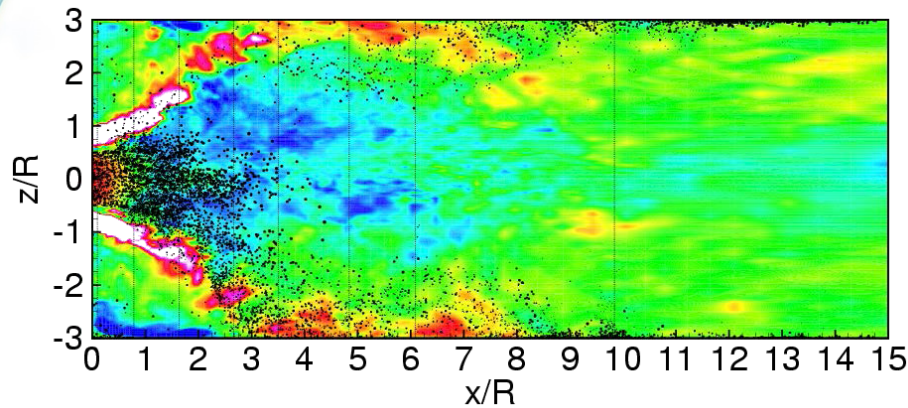


	Case 1	Case 2
Reynolds Number	26,200	27,250
Swirl Number	0.47	0.49
Loading Ratio	0.034	0.17 (5x)
Density Ratio	2152	

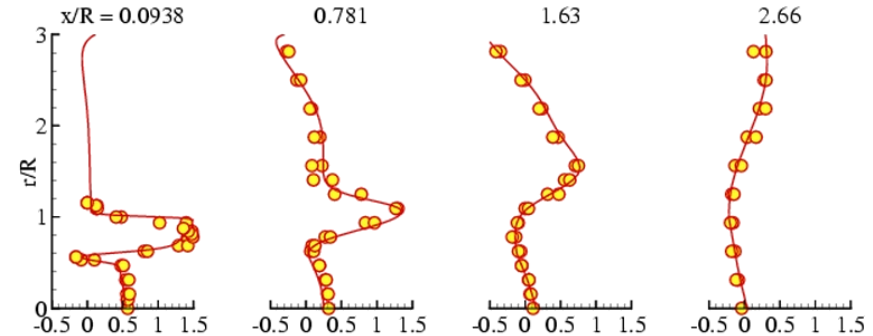
$R_{\text{ref}} = 32 \text{ mm}$, $U_{\text{ref}} = 12.9 \text{ m/s}$



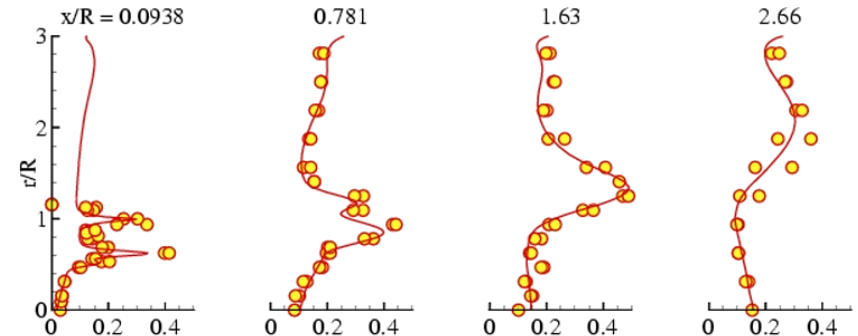
Predictive accuracy demonstrated in complex flows with no model tuning



Mean Profiles:

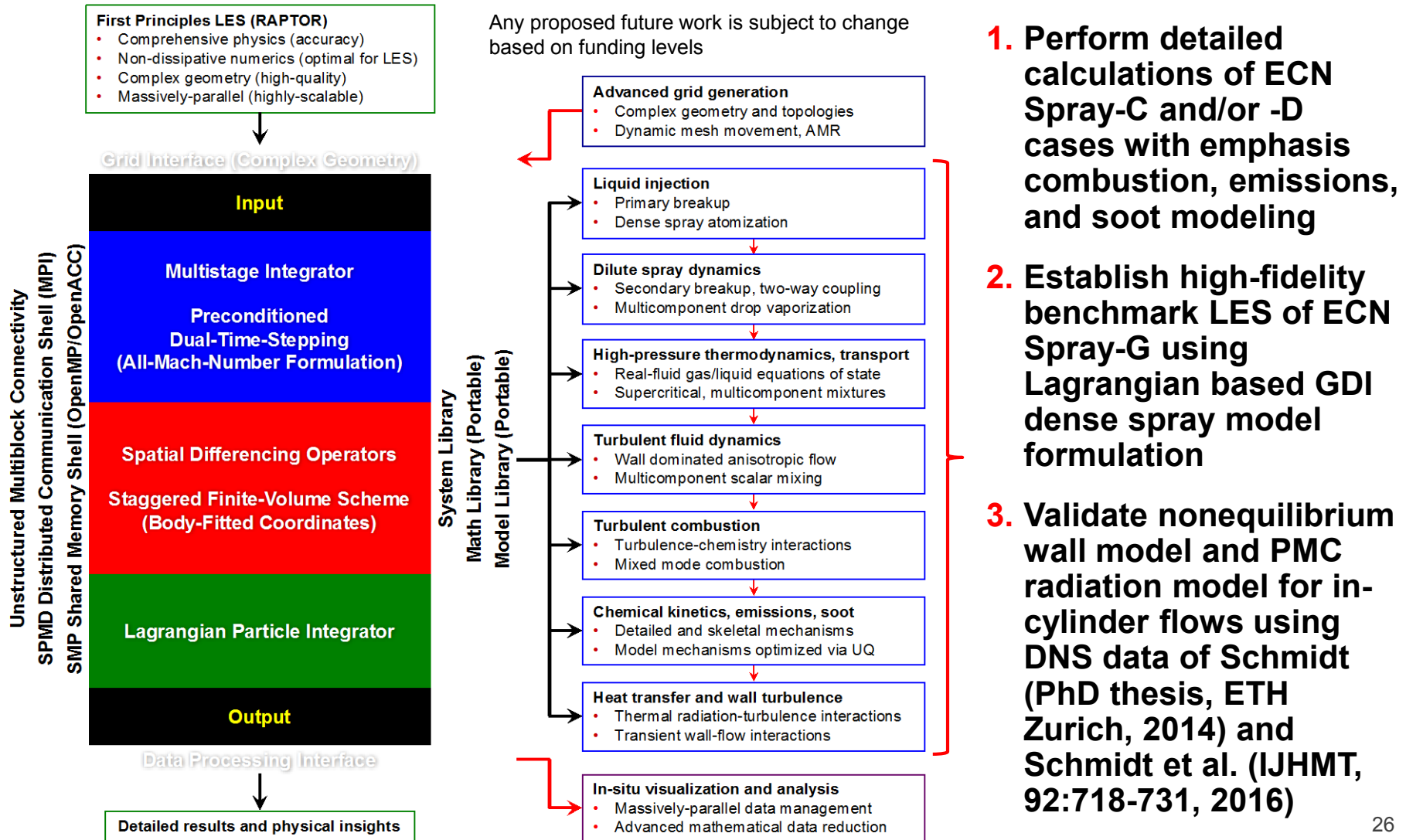


RMS Profiles:



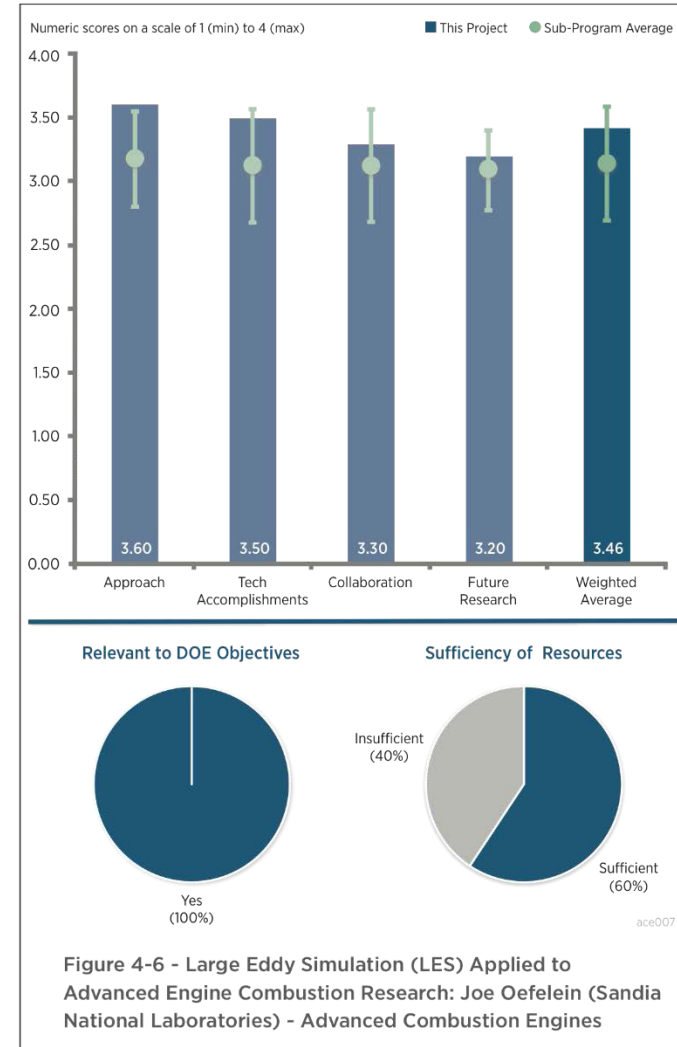
Time-averaged particle mean and RMS velocity profiles show good agreement with experimental measurements in a model axisymmetric combustor configuration

Proposed future work ... establish detailed benchmarks as follows ...



Response to previous year reviewer comments

- **Comment:** Approach of developing and applying detailed first principles models for the wide range of complex in-cylinder processes is excellent. However, progress to combine these into an all-up simulation of a diesel or GDI engine has yet to be achieved (although progress toward this goal is measurable).
- **Response:** It is important to recognize the numerous challenges required to develop advanced flow solvers and use them to perform detailed calculations on state of the art computer architectures. We are working toward full engine geometries. Code has the capability. The current rate limiting factor is funding level and related staffing. Given this, our focal point is to provide reference simulation data, not a software tool for engine design.
- **Comment:** Good coordination with government laboratories and academia. Would like to see more interaction with industry.
- **Response:** We are attempting to establish closer interactions. Our goal is to complement what current commercial/industry design codes already provide, not reproduce more of the same. This involves providing data and insights not available from experiments and developing the collaborative workflow required to overcome the major obstacles for development of predictive models. The major bottleneck is the time and labor required to obtain solutions.
- **Comment:** All reviewers would like to see faster progress. Many reviewers stated project appears to be limited in funding.
- **Response:** We have attempted to build the team up over time by hiring staff. However, this has been stalled over the past few years due to funding cuts. Current spend plan is now \$260K.





Collaboration and coordination with other institutions

- **ORNL-OLCF, Center for Accelerated Application Readiness (CAAR)**
 - **CAAR Partnership in Turbulent Combustion using the RAPTOR Code Framework: Application Readiness and Early Science on next generation leadership class platform (called SUMMIT)**
- **Penn State (Haworth), U Michigan (Sick), ORNL (Szybist)**
 - **Development and Validation of Predictive Models for In-Cylinder Radiation and Wall Heat Transfer**
- **Penn State (Haworth), U Merced (Modest)**
 - **Turbulence-Radiation Interactions in Reacting Flows: Effects of Radiative Heat Transfer on Turbulence**
- **Stanford (Ihme), U Michigan (Sick)**
 - **Development of a Dynamic Wall Layer Model for LES of Internal Combustion Engines**
- **CERFACS (Poinsot et al.)**
 - **Numerical Benchmarks and comparisons of High-Pressure High-Reynolds-Number Turbulent Reacting Flows using the AVBP and RAPTOR Codes**

Remaining challenges and barriers

... developing an optimal workflow for model V&V

Basic Research

Specialized Research Code, Expert User/Developer

- Maximum accuracy/fidelity, unique use of leadership class platforms
- Comprehensive physics (accuracy)
- Optimal numerics; e.g., nondissipative
- Massively-parallel and scalable

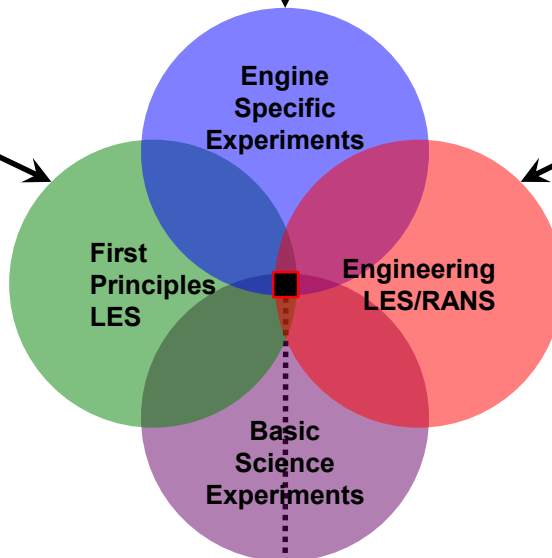
Phenomenological Drivers

- High-Reynolds-number turbulence
- High-pressure mixed-mode combustion
- Compressible, acoustically active flow
- Complex geometry, heat transfer
- Complex fuels, multiphase flow

Engineering CFD

Professionally Supported Design Tool, Broad User Population

- Fast solution turn-around, optimal balance between cost and accuracy
- Essential physics (cost vs. accuracy)
- Robust resilient numerics
- Minor parallelism and scalability



GOAL

Provide data required for detailed assessment of design codes

Joint Analysis of Common Target Cases

GOAL

Expand envelope of confidence and accuracy of design codes

Predictive Models

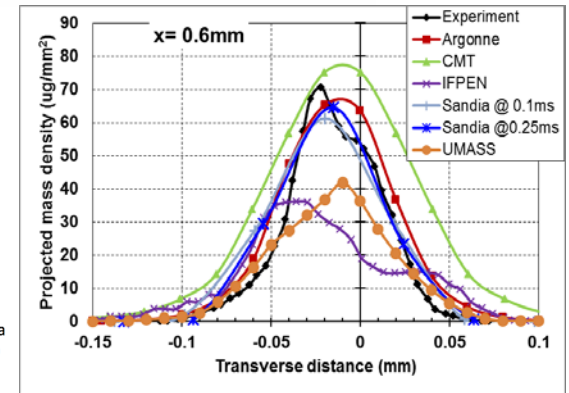
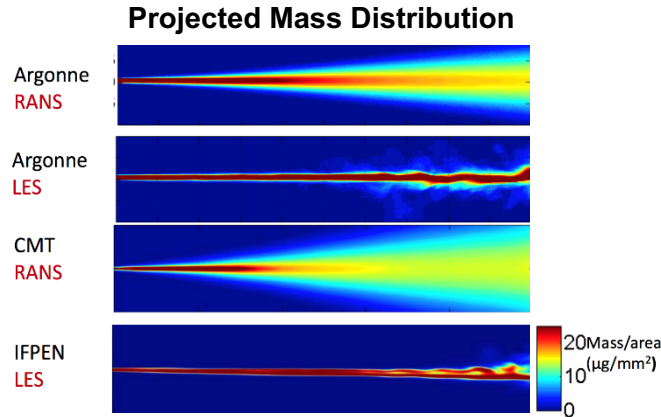
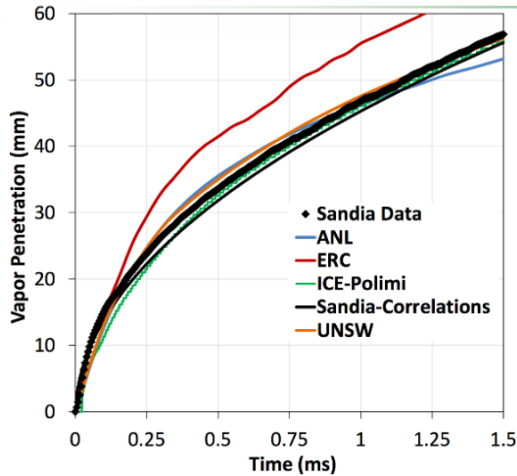
Summary

- **Highlighted typical inconsistencies in model development using Spray-A case as example and focused on effects of detailed thermodynamics and transport**
 - Performed comparisons with available experimental data, then analyzed the dynamics of the transient mixing field and state just prior to autoignition
 - Scalar-mixing is significantly modified by non-ideal multicomponent thermodynamics (e.g., flow locally supersonic in mixing layer due to variations in sound speed)
- **Quantified effects of broadband transient mixing on development of flammable regions just prior to autoignition as function of P, T, and equivalence ratio**
 - e.g., for Spray-A, localized pockets of flammable mixture form between 200 and 250 diameters downstream of the injector (consistent with experiments)
 - Results facilitate development of optimal autoignition models based on simplified chemical model and related combustion closure
- **Demonstrated the wide variability exists between leading detailed and skeletal chemical mechanisms, applied UQ methods to derive “optimal” chemical model**
 - None of the available mechanisms have been developed for pressures typically encountered in for propulsion and power systems (e.g., all designed for ≤ 20 bar)
 - Detailed characterization of variability across key operational envelopes important (e.g., “Optimal” chemical model provides balance between cost and accuracy)
- **Demonstrated a collaborative approach that combines UQ, experiments, and simulations in situations where detailed data for model validation is sparse**



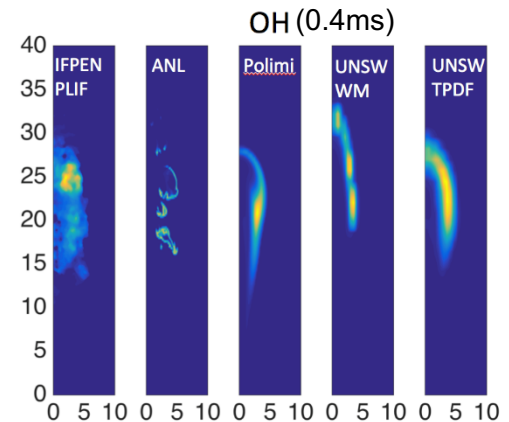
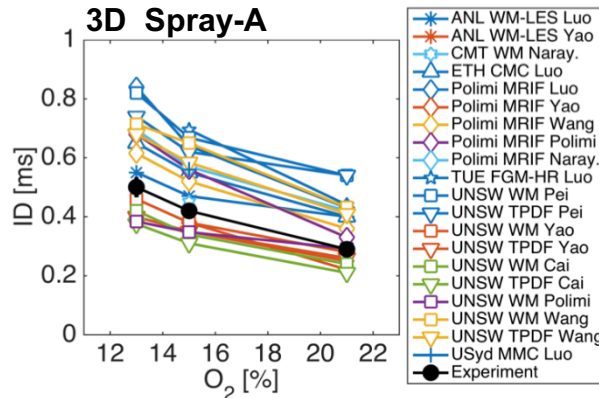
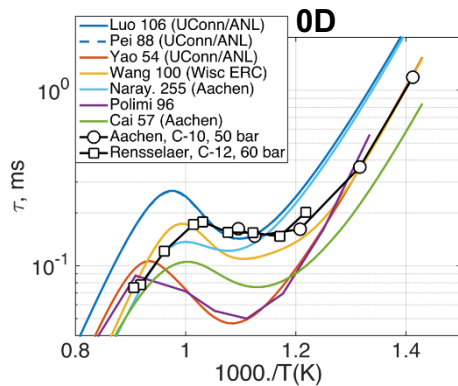
Technical Back-Up Slides

Deficiencies in model development have been demonstrated for years



Inconsistencies in non-reacting calculations observed in all ECN workshops (here ECN4)

- Correct vapor penetration but large scatter in other quantities



Similarly, large scatter is observed in reacting calculations

- Large variability between chemical mechanisms and shock tube data, and scatter in ignition delay (ID) in Spray-A simulations

There is a distinct lack of discriminating data due to many competing effects in both models and numerical methods ...

Filtered conservation equations

- Mass:

$$\frac{\partial}{\partial t}(\theta \bar{\rho}) + \nabla \cdot (\theta \bar{\rho} \tilde{\mathbf{u}}) = \bar{\dot{\rho}}_s$$

- Momentum:

$$\frac{\partial}{\partial t}(\theta \bar{\rho} \tilde{\mathbf{u}}) + \nabla \cdot \left[\theta \left(\bar{\rho} \tilde{\mathbf{u}} \otimes \tilde{\mathbf{u}} + \frac{\mathcal{P}}{M^2} \mathbf{I} \right) \right] = \nabla \cdot (\theta \vec{\tau}) + \bar{\mathbf{F}}_s$$

- Total Energy:

$$\frac{\partial}{\partial t}(\theta \bar{\rho} \tilde{e}_t) + \nabla \cdot [\theta (\bar{\rho} \tilde{e}_t + \mathcal{P}) \tilde{\mathbf{u}}] = \nabla \cdot \left[\theta \left(\vec{Q}_e + M^2 (\vec{\tau} \cdot \tilde{\mathbf{u}}) \right) \right] + \theta \bar{Q}_e + \bar{Q}_s$$

- Species:

$$\frac{\partial}{\partial t}(\theta \bar{\rho} \tilde{Y}_i) + \nabla \cdot (\theta \bar{\rho} \tilde{Y}_i \tilde{\mathbf{u}}) = \nabla \cdot (\theta \vec{S}_i) + \theta \bar{\dot{\omega}}_i + \bar{\dot{\omega}}_{s_i}$$

- Spray Source Terms
- Composite Stresses/Fluxes
- Chemical Source Terms

Mixed dynamic Smagorinsky model for turbulence and scalar mixing

- Eddy Viscosity:

$$\mu_t = \bar{\rho} C_R \Delta^2 \Pi_{\tilde{\mathbf{S}}}^{\frac{1}{2}} \quad \Pi_{\tilde{\mathbf{S}}} = \tilde{\mathbf{S}} : \tilde{\mathbf{S}} \quad \tilde{\mathbf{S}} = \frac{1}{2} (\nabla \tilde{\mathbf{u}} + \nabla \tilde{\mathbf{u}}^T)$$

- Stress Tensor:

$$\vec{\mathcal{T}} = (\bar{\boldsymbol{\tau}} - \mathbf{T}) = (\mu_t + \mu) \frac{1}{Re} \left[-\frac{2}{3} (\nabla \cdot \tilde{\mathbf{u}}) \mathbf{I} + (\nabla \tilde{\mathbf{u}} + \nabla \tilde{\mathbf{u}}^T) \right] - \bar{\rho} \left(\widetilde{\tilde{\mathbf{u}} \otimes \tilde{\mathbf{u}}} - \tilde{\mathbf{u}} \otimes \tilde{\mathbf{u}} \right) - \frac{1}{3} \bar{\rho} q_{\text{sfs}}^2 \mathbf{I}$$

- Energy Flux:

$$\vec{\mathcal{Q}}_e = (\bar{\mathbf{q}}_e - \mathbf{Q}) = \left(\frac{\mu_t}{Pr_t} + \frac{\mu}{Pr} \right) \frac{1}{Re} \nabla \tilde{h} + \sum_{i=1}^N \tilde{h}_i \vec{\mathcal{S}}_i - \bar{\rho} \left(\widetilde{\tilde{h} \tilde{\mathbf{u}}} - \tilde{h} \tilde{\mathbf{u}} \right)$$

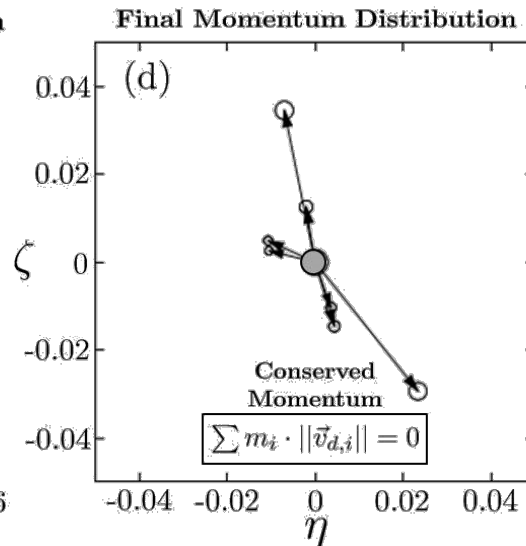
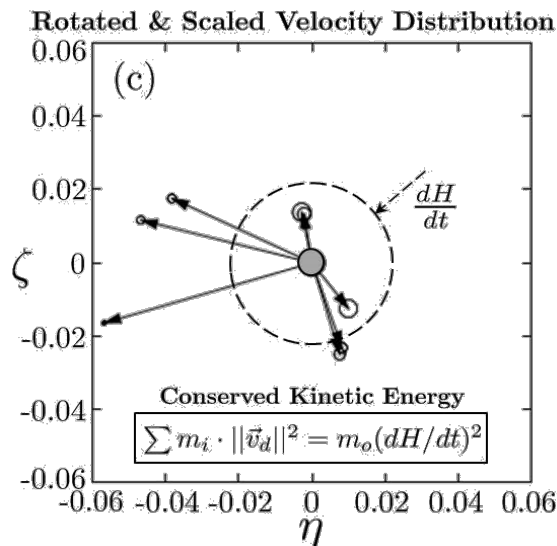
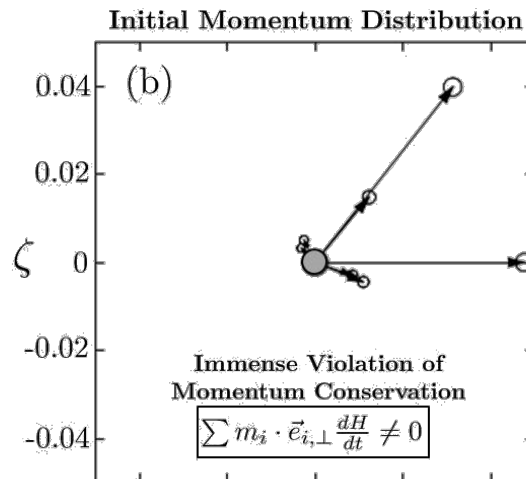
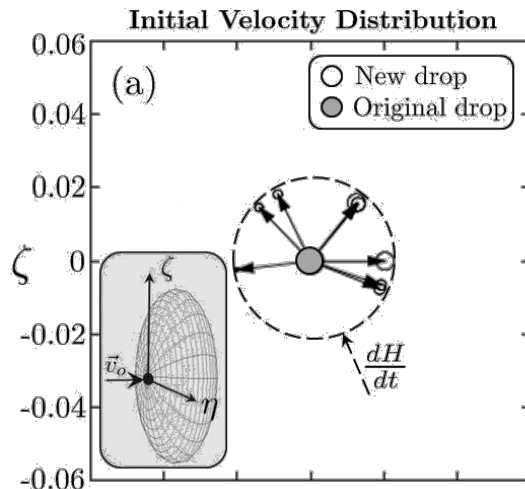
- Mass Flux:

$$\vec{\mathcal{S}}_i = (\bar{\mathbf{q}}_i - \mathbf{S}_i) = \left(\frac{\mu_t}{Sc_{t_i}} + \frac{\mu}{Sc_i} \right) \frac{1}{Re} \nabla \tilde{Y}_i - \bar{\rho} \left(\widetilde{\tilde{Y}_i \tilde{\mathbf{u}}} - \tilde{Y}_i \tilde{\mathbf{u}} \right)$$

Coefficients C_R , Pr_t , and Sc_{t_i} evaluated dynamically as functions of space and time

Improved breakup model also derived that conserves momentum

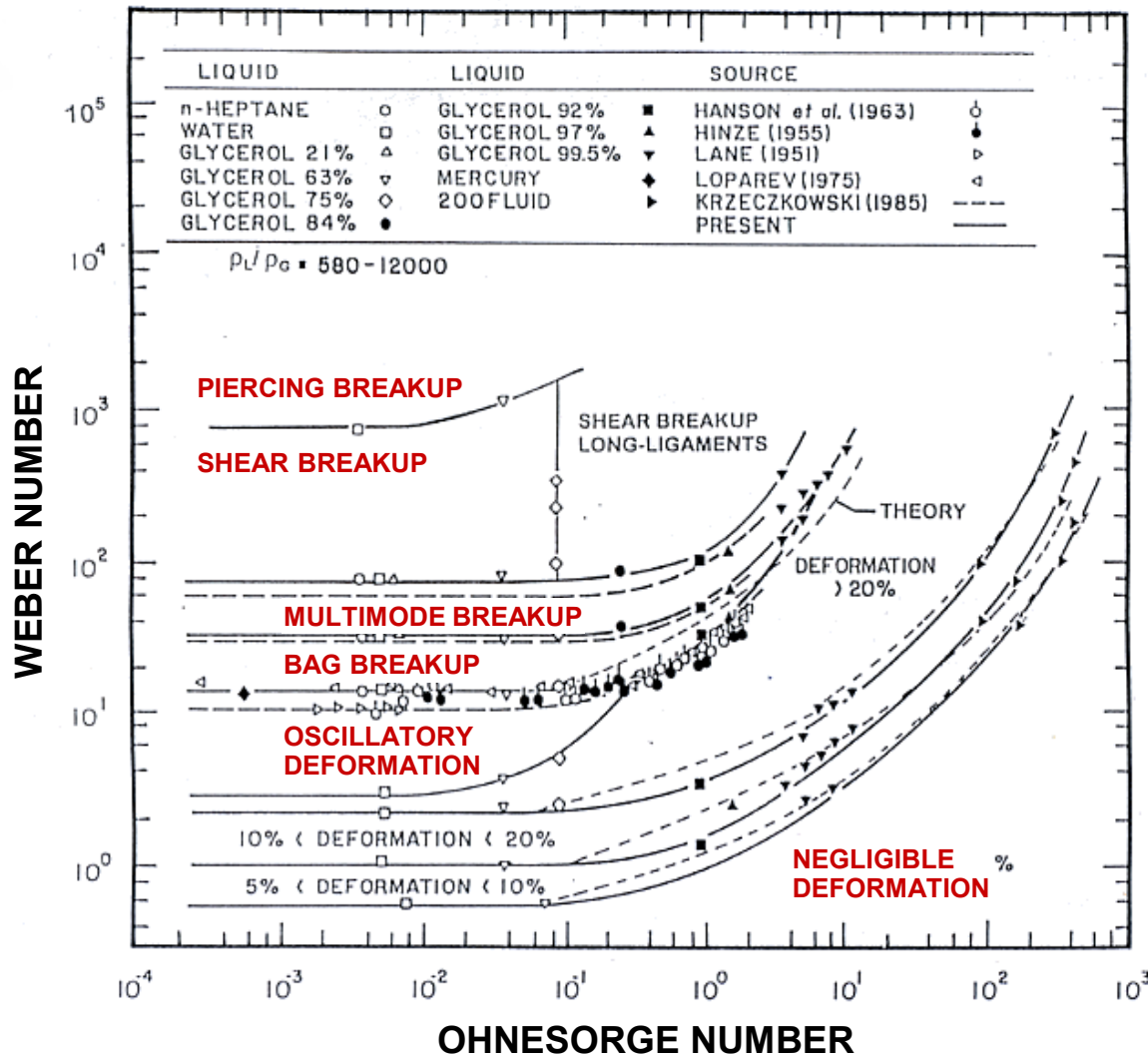
Classic Framework
↕
New Framework



Normalized drop velocity and momentum distributions

- a) Initial drop velocity distribution
- b) Corresponding momentum distribution after multiplication of the velocities in (a) with the respective drop masses (Momentum contributions do not cancel, thus momentum conservation is significantly violated)
- c) Drop velocity distribution after rotation of the initial solution in (a) to enforce momentum conservation and scaling to maintain energy conservation
- d) Conserved momentum distribution after the rotation and scaling operation

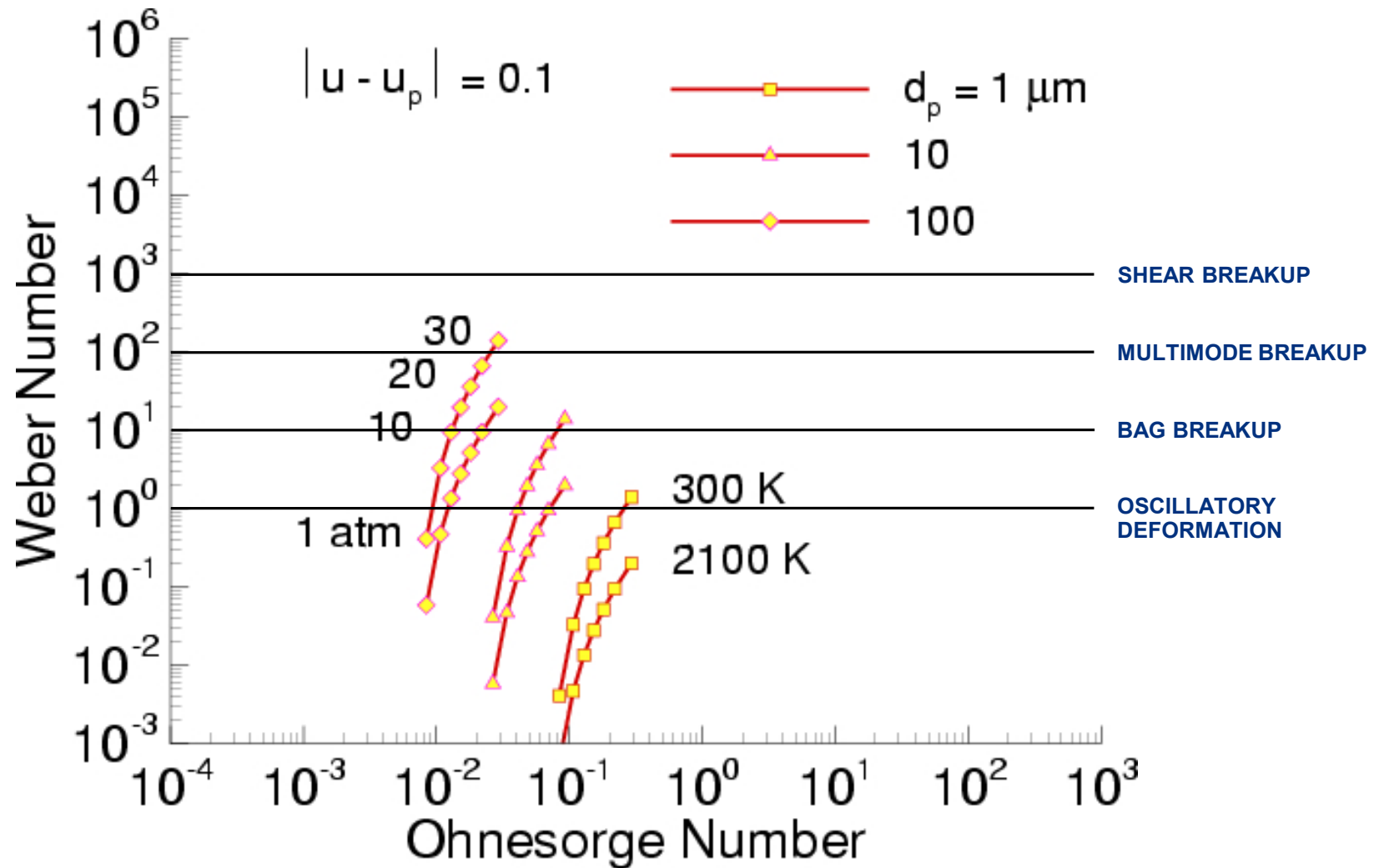
Results being used to understand what regimes models must perform over



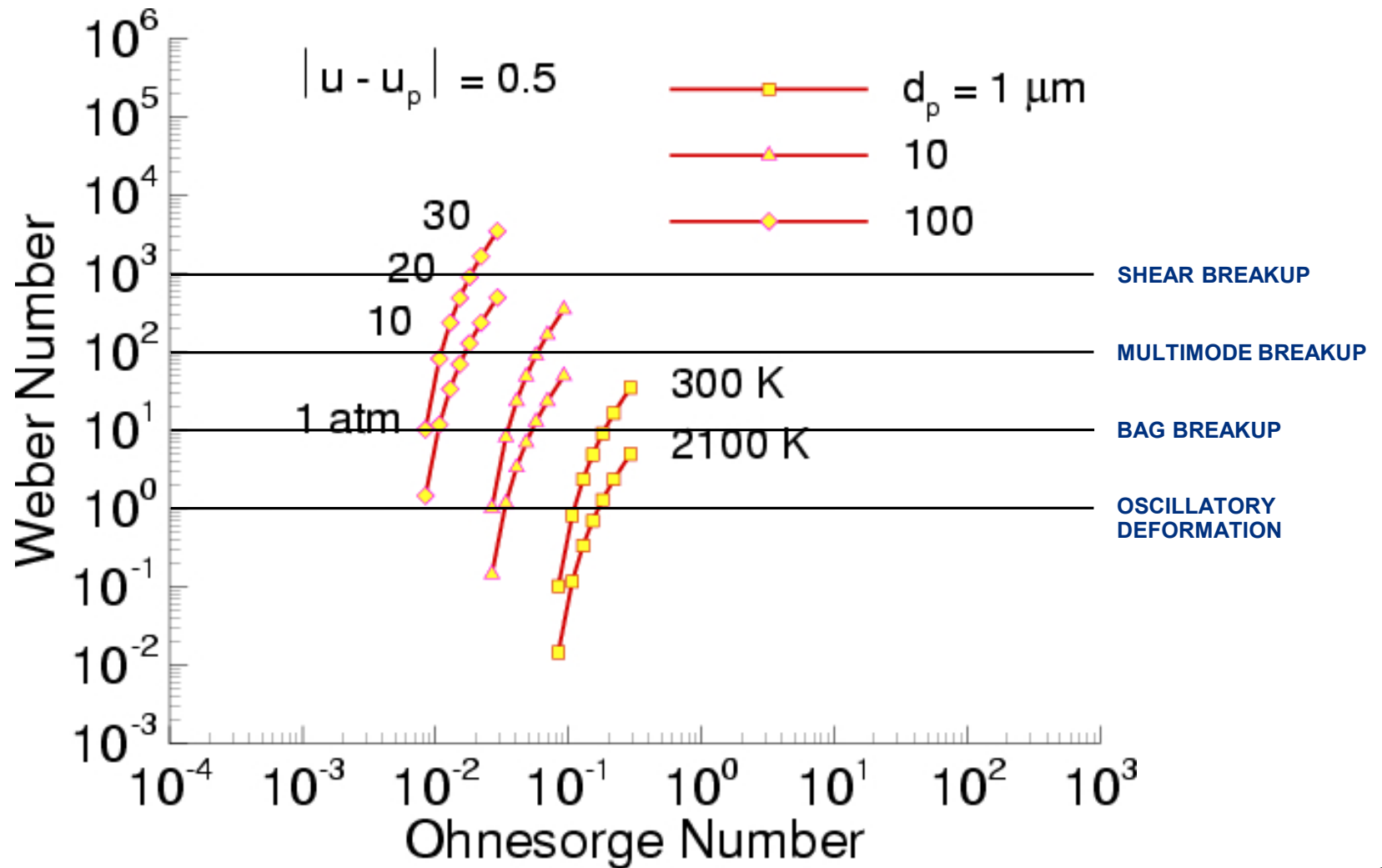
Drop deformation and secondary breakup regimes

Hsiang and Faeth, International Journal of Multiphase Flow, 18:635-652, 1992

Relevant deformation and secondary breakup regimes



Relevant deformation and secondary breakup regimes





End